

Využití metod dielektrické spektroskopie pro diagnostiku průběhu vybraných síťovacích reakcí

Stanislav Pištěk

Master thesis
2008



Tomas Bata University in Zlín
Faculty of Applied Informatics

Univerzita Tomáše Bati ve Zlíně
Fakulta aplikované informatiky
Ústav automatizace a řídicí techniky
akademický rok: 2007/2008

ZADÁNÍ DIPLOMOVÉ PRÁCE

(PROJEKTU, UMĚLECKÉHO DÍLA, UMĚLECKÉHO VÝKONU)

Jméno a příjmení: **Bc. Stanislav PIŠTĚK**
Studijní program: **N 3902 Inženýrská informatika**
Studijní obor: **Automatické řízení a informatika**

Téma práce: **Využití metod dielektrické spektroskopie pro diagnostiku průběhu vybraných síťovacích reakcí.**

Zásady pro vypracování:

1. Vypracujte literární rešerši popisující současný stav dané problematiky.
2. Seznamte se s programovacím prostředím Agilent VEE PRO a vytvořte v něm vhodný algoritmus pro měření v reálném čase.
3. Provedte experimentální měření síťování epoxidových pryskyřic metodou dielektrické spektroskopie.
4. Provedte stejné měření pro síťovací reakci hydrolyzovaného kolagenu s glutaraldehydem.
5. Zaměřte se na měření disipačního faktoru a prozkoumejte vliv teploty na průběh síťovací reakce.
6. Vyhodnoťte výsledky experimentů a navrhněte možnosti pokračování pro oblast zkoumání kinetiky síťovací reakce hydrolyzovaného kolagenu.

Rozsah práce:

Rozsah příloh:

Forma zpracování diplomové práce: **tištěná/elektronická**

Seznam odborné literatury:

1. **Stanislav Ďaďo, Marcel Kreidl: Senzory a měřicí obvody, Vydavatelství ČVUT, Praha 1996**
2. **Fraden Jacob: Handbook of Modern Sensors: Physics, Designs, and Applications, 2nd ed. New York, Springer Verlag, 1996**
3. **HEDVIG, P.: Dielectric Spectroscopy of Polymers, AKADEMIAI KIADO Budapest 1977**
4. **Proc. Polymer science, Epoxy Resins and Composites IV, Akademie-Verlag Berlin 1987**
5. **Navrátil Milan: Instrumentace a zpracování signálů při měření kinetiky síťovacích reakcí pomocí impedanční spektroskopie, Diplomová práce, 2002, UTB Zlín.**

Vedoucí diplomové práce:

Ing. Milan Navrátil, Ph.D.

Ústav elektrotechniky a měření

Datum zadání diplomové práce:

22. února 2008

Termín odevzdání diplomové práce:

6. června 2008

Ve Zlíně dne 22. února 2008



prof. Ing. Vladimír Vašek, CSc.
děkan



prof. Ing. Vladimír Vašek, CSc.
ředitel ústavu

ABSTRAKT

Tato práce se zabývala zkoumáním změn dielektrických vlastností během procesu síťování u vybraných chemických reakcí. Byla zaměřena na zkoumání epoxidových pryskyřic a hydrolyzovaného kolagenu, který byl síťován glutaraldehydem. Předmětem zkoumání byly faktory jako teplota a frekvence, jež ovlivňují reakci.

Klíčová slova: dielektrická spektroskopie, hydrolyzovaný kolagen, epoxid, glutaraldehyd

ABSTRACT

The purpose of this diploma thesis was examination of time behavior of dielectric values measured during cross-linking reaction of chosen chemical systems. It was considered to the examination of epoxide resin and hydrolyzed collagen cross-linked by glutaraldehyde. The main factors influencing the reaction such as frequency and temperature were the point of attention.

Keywords: dielectric spectroscopy, hydrolyzed collagen, epoxy resins, glutaraldehyde

ACKNOWLEDGEMENTS

This master thesis could not have been written without Milan Navrátil's help, who served me as my supervisor and gave me lots of good advices. He and the other faculty members patiently guided me through the study. I thank them all

CONTENTS

INTRODUCTION	7
I. THEORY	8
1 COLLAGEN	9
1.1 HYDROLYZED COLLAGEN	11
2 BASIC PRINCIPLES OF DIELECTRIC SPECTROSCOPY	12
2.1 ADMITTANCE MEASUREMENT	13
2.2 DISSIPATION FACTOR	16
2.3 DIELECTRIC CONDUCTION MECHANISMS (IN BULK MATERIALS)	17
2.4 IONIC CONDUCTIVITY	18
2.5 DIPOLE ORIENTATION	19
3 ULTRAVIOLET-VISIBLE SPECTROSCOPY	22
II. ANALYSIS	26
4 HARDWARE	27
4.1 HEWLETT PACKARD 4284A PRECISION LCR METER	27
4.2 TECHNOLOGICAL CARD NI-488.2	27
4.3 MEMMERT UNIVERSAL OVEN MODEL UNP 200	28
4.4 HELIOS ALPHA SPECTROPHOTOMETER	30
5 SOFTWARE	31
5.1 AGILENT VEE 8.0	31
6 MEASURING WORKSPACE AND ITS PREPARATION	32
6.1 USER APPLICATIONS IN VEE PRO	32
6.1.1 Application for measuring of dissipation factor.....	32
6.1.2 Application for quick displaying saved data	34
6.2 DIELECTRIC SPECTROSCOPY METHOD.....	35
6.2.1 Epoxy resin.....	36
6.2.2 Hykol.....	38
7 SPECTROPHOTOMETRIC MEASUREMENT OF ABSORBANCE	42
CONCLUSION	45
BIBLIOGRAPHY	47
LIST OF ABBREVIATIONS	48
LIST OF FIGURES	50
LIST OF TABLES	52
LIST OF APPENDICES	53

INTRODUCTION

The first application of dielectric spectroscopy was published by Kiele and Race in 1934. They described usage of this method for study polyesterification reactions. Many research papers have been written since 1958, most of them dealt with epoxy resins, less about polyesters, polyamides and other resins. Progress in this field was mainly caused by industry needs especially aeronautics. Next but not less important fact was improvement in measurement devices. Here are some important facts:

- At the low frequencies the polarization is being applied.
- Ionic conductivity is the best for monitoring of dielectric properties.
- AC or DC current doesn't have an effect on conductivity
- Conductivity and viscosity are linked together at the beginning of reaction

The work on this issue has begun by Milan Navrátil in 2002 [1]. The complete measuring workplace has been created. But that work described influence of temperature on cross-linking reactions only marginally.

Thus the goal of this work is examination of cross-linking reaction in dependence on temperature and frequency.

I. THEORY

1 COLLAGEN

Collagen is a protein which is main component of bones, skin, sinews and tissue, making up about 25% of the total protein content. It has characteristic composition of amino acids and spatial sequence.

Glycine is a main component of collagen's molecule it can contain up to 28%. Little bit less significant part is proline (about 15%).

A lot of scientists have been working on collagen structure for a long time. Some of them were Nobel prize laureates like Watson and Crick and Linus Pauling. The triple helical structure that is known to be correct in the essentials was proposed by G. N. Ramachandran and Gopinath Kartha in the year 1954. This proposed structure came to be known as the Madras helix.

The tropocollagen or so-called collagen molecule subunit is a rod about 300 nm long and 1.5 nm in diameter, consist of three polypeptide strands, each of them is a left-handed helix. A triple helix is created by three left-handed helices which are twisted together into one right-handed coiled coil, a cooperative quaternary structure stabilized by numerous hydrogen bonds. Tropocollagen subunits spontaneously self-assemble, with regularly staggered ends, into even larger arrays in the extra cellular spaces of tissues. There is some covalent cross-linking within the triple helices, and a variable amount of covalent cross-linking between tropocollagen helices, to form the different types of collagen found in different mature tissues — similar to the situation found with the α -keratins in hair. Collagen's insolubility was a barrier to study until it was found that tropocollagen from young animals can be extracted because it is not yet fully cross-linked. [3]

Collagen fibrils are collagen molecules packed into an organized overlapping bundle. Collagen fibers are bundles of fibrils.

Because glycine is the smallest amino acid, it plays a unique role in fibrous structural proteins. In collagen, Gly is required at every third position because the assembly of the triple helix puts this residue at the interior (axis) of the helix, where there is no space for a larger side group than glycine's single hydrogen atom. For the same reason, the rings of the Pro and Hyp must point outward. These two amino acids thermally stabilize the triple helix — Hyp even more so than Pro — and less of them is required in animals such as fish, whose body temperatures are low.[3]

Collagen is mainly being used in leather industry for crop production. But it has other applications, especially in medicine due to similarity with human body collagen and its ability to absorb water. The review can be found in Table 1.

Structure	Area of Usage / products
flat (netting)	leather production, wound coverage, skin replacement, vessel replacement
Fibers	artificial casing, packing foils, membranes, wound powder
Fibrils	biocompatible materials, bone surgery
Macromolecule	native collagen, atelocollagen, desamido-collagen for cosmetics purpose
Polypeptides	gelatin, fish-glue, hydrolysate, plasma expanders, pills capsule, tensids, emulgators, thickener, feed, fertilizer

Table 1. Hierarchy according to structure and area of usage [1]

1.1 Hydrolyzed collagen

Research is being concerned to enzymatic hydrolysis of proteins. Higher temperatures are needed for this process because native collagen can resist to proteolytic enzymes if the temperature is not high enough. Higher temperature causes that the secondary structure of collagen will apart and in consequence of this peptides segments become accessible. [4]

Amino Acids	Hydrolyzed collagen	Collagen
Glycin	33	32,7
Prolin	12,5	13
Hydroxyprolin	10	8,6
Alanin	8,4	11,4
Glutamic acid	7,7	7,5
Asparatic acid	5,1	4,6
Arginin	4,8	5,2
Serin	4,1	3,1

Table 2. Percentage volume of main amino acids in hydrolyzed collagen and collagen [1]

2 BASIC PRINCIPLES OF DIELECTRIC SPECTROSCOPY

The interaction between electromagnetic radiation and electric dipole movement allows test materials by dielectric spectroscopy. The frequencies from 10^{-6} Hz to 10^{10} Hz are being used for testing. Under 10^{-6} Hz the contribution of the induced dipole moments becomes small in contrast with that of the permanent dipole moments of the system. Over 10^{10} Hz, in the infrared optical and ultraviolet area, the absorption and emission of radiation is due to changes in the induced dipole moments, which are dependent on the polarizability of the atoms or molecules. Thus studying polar molecules in the gaseous phase or in liquids is main area of usage of dielectric spectroscopy because the radiation is absorbed here mainly by the reorientation of permanent dipoles. This method was introduced by Debye in 1931 and is being used to determine molecular dipole movement.

The situation is more complicated in the condensed phase due to the electronic states of the system cannot be determined by term of molecular orbitals collective crystal states (excitons) are to be considered. Rice and Jortner proved in 1967 that the dielectric behaviour of solid can be correctly interpreted only by terms of excited state thence it follows that induced dipole moments can contribute to the absorption of radiation appreciably even at the low frequency range. Also intermolecular interactions have a strong impact to the dipole moments of molecules. These interactions can be described in terms of exciton states.

In the materials like polymeric solids and visco-elastic fluids the donation of the exciton states to the permanent dipole moments is quite small at any rate is not strong enough to consider certain groups of atoms or bonds individually. In the basic state appropriately one can observe a polymeric solid having certain polar groups at primary approximation as a system of weakly interacting electrical dipoles. This method of dielectric spectroscopy is primarily targeted to gases and solutions but it can also be used to polymeric solids with less or more accuracy. Recently, attention is paid to the effect of induced dipole polarization in polymers, which is directly connected with the exciton states and subsequently with the physical structure of the solid.

The response of a material to an peripheral electric field is basically a statistical effect. The observation of the orientation of all individual moments is impossible. Only the bulk polarization of the material can be determined. Pursuant to this fact can be told that dielectric spectroscopy is based on statistical thermodynamical deliberations. [2]

2.1 Admittance Measurement

Tested material is placed between two electrodes which are connected to source of alternating current (AC) as is shown on the Fig. 1. AC will create electric field and tested material will be polarized, and thus became conductive.

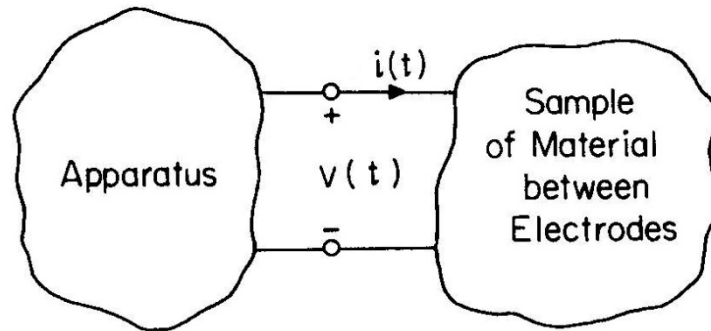


Fig. 1. Apparatus applies a time-varying voltage $u(t)$ to the electrodes and measures the time varying current $i(t)$ [4]

Behavior of current $i(t)$ and voltage $v(t)$ can be defined like:

$$u(t) = U_0 \cos(\omega t) \quad (1)$$

$$i(t) = I_0 \cos(\omega t + \varphi) \quad (2)$$

where ω is angular frequency, $i(t)$ and $v(t)$ has sinusoidal wave. Also there is phase difference φ between them. $I_0(t)$ and $V_0(t)$ are maximal amplitudes.

This is displayed on the next Fig. 2.

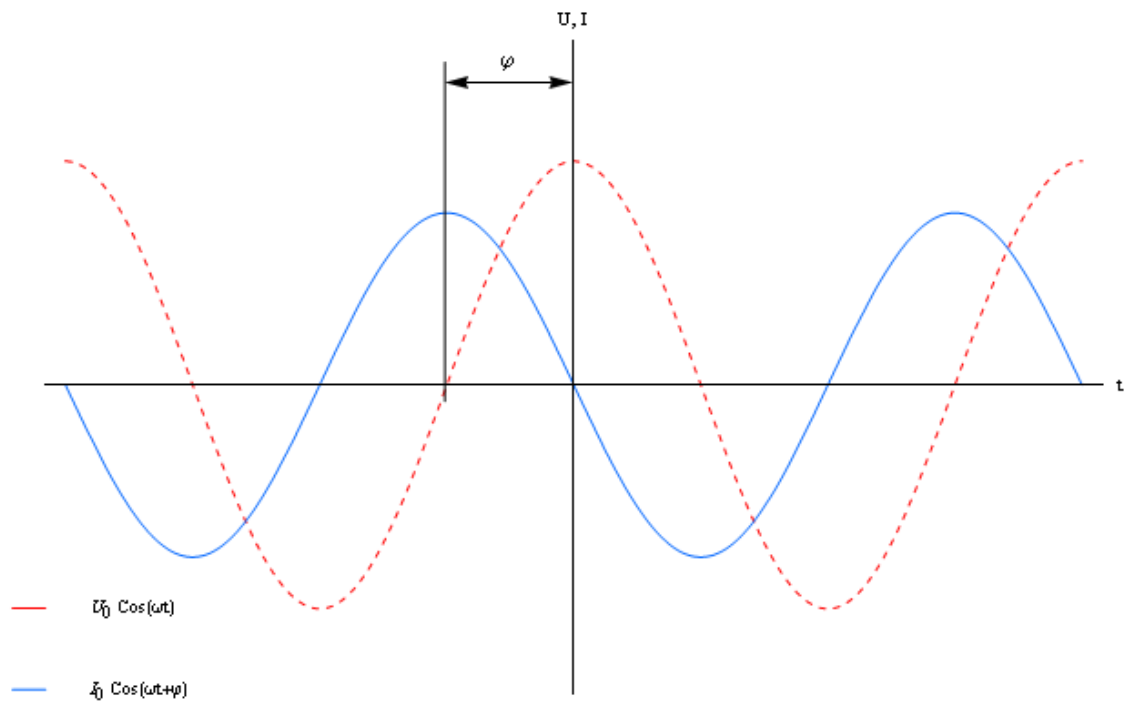


Fig. 2. Sinusoidal voltage and current waveforms having a phase difference ϕ

Preceding formulas (1), (2) can be expressed in complex exponential notation:

$$u(t) = \operatorname{Re}\{Ue^{j\omega t}\} \quad (3)$$

$$i(t) = \operatorname{Re}\{Ie^{j\omega t}\} \quad (4)$$

where j is $(-1)^{1/2}$, U and I are the complex amplitudes of $v(t)$ and $i(t)$. When expressed in this form:

$$U = U_0 \quad (5)$$

$$I = I_0 e^{j\varphi} \quad (6)$$

Admittance is defined like:

$$Y(\omega) = \frac{I}{U} = \frac{1}{Z(\omega)} \quad (7)$$

after substitution:

$$Y(\omega) = j(I_0 / U_0) \sin \varphi + (I_0 / U_0) \cos \varphi \quad (8)$$

In (8), the phase φ and the amplitude of the admittance (I_0/U_0) depend on frequency. But at some frequency equivalent electric circuit consists of resistor $R_x(\omega)$ and capacitor $C_x(\omega)$ parallel-connected can be use. This circuit can be seen in the next Fig. 3

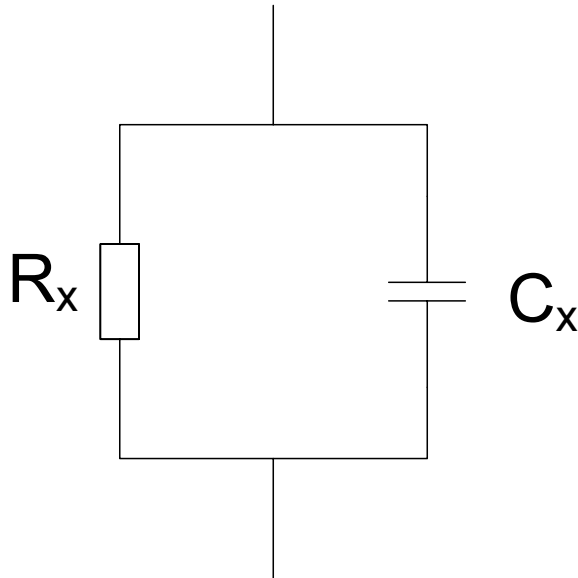


Fig. 3. Equivalent circuit for the admittance of the electrodes and sample

For parallel RC circuit from Fig. 3 can be admittance expressed like:

$$Y(\omega) = j\omega C_x(\omega) + R_x^{-1} \quad (9)$$

next step is comparing of (8) to (9), now R_x and C_x can be expressed

$$R_x = \frac{U_0}{I_0 \cos \varphi} \quad (10)$$

$$C_x(\omega) = \frac{I_0 \sin \varphi}{\omega U_0} \quad (11)$$

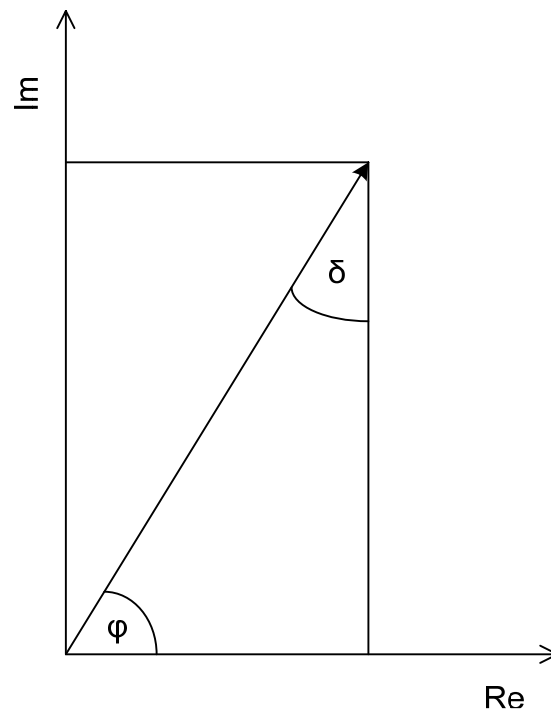


Fig. 4. Impedance in the complex plane

Total impedance of RC circuit in the Fig. 3 can be expressed by following equation

$$\frac{1}{Z} = \frac{1}{X_{C_x}} + \frac{1}{R_x} \quad (12)$$

where

$$X_{C_x} = \frac{1}{j\omega C_x} \quad (13)$$

from Eqs. (12) and (13) can be expressed

$$Z = \frac{R_x}{1 + j\omega R_x C_x} = \frac{R_x}{1 + \omega^2 R_x^2 C_x^2} - j \frac{\omega R_x^2 C_x}{1 + \omega^2 R_x^2 C_x^2} \quad (14)$$

2.2 Dissipation factor

Dissipation factor D is common used quantity in admittance measurement. It is phase dependent on admittance. Its magnitude does not affect.

$$D = \frac{1}{\omega R_x C_x} \quad (15)$$

which from Eqs. (10) and (11), yields

$$D = \cotg(\varphi) = \tg(\delta) \quad (16)$$

because following Eqs. exist

$$R = \rho \frac{l}{S} \quad (17)$$

$$C = \varepsilon \frac{S}{l} \quad (18)$$

$$\sigma = \frac{1}{\rho} \quad (19)$$

where σ is electrical conductivity and has the SI units of siemens per meter [$\text{S}\cdot\text{m}^{-1}$], ρ is the static resistivity of the material in [$\Omega\cdot\text{m}$], ε is permittivity which is measured in farads per meter [F/m]

by substituting (17), (18), (19) into (15) yields

$$D = \frac{1}{\omega RC} = \frac{\sigma}{\omega \varepsilon} \quad (20)$$

From the Eq.(20) cited above can be obvious that D depends only on angular frequency, permittivity and conductivity.

Next useful quantity is loss tangent which is equal to dissipation factor D

$$\tg \delta_x = D \quad (21)$$

consequently

$$\delta_x = \pi/2 - \varphi \quad (22)$$

2.3 Dielectric conduction mechanisms (in bulk materials)

The permittivity ε' can be written as

$$\varepsilon' = \varepsilon_\infty + \varepsilon_d'$$

where ε_∞ is base line permittivity and ε_d' is additional permittivity attributed to dipole orientation and it is dependent on frequency, temperature and level of crosslinking of material.

2.4 Ionic conductivity

The importance of ionic conductivity in curing resins has been proved in many earliest works. Ionic conductivity is mainly caused by free ions, especially chlorine and sodium ions. They are produced like minor products in polymerization reactions.[4]

Electric field with intensity \vec{E} causes that ions in material have average drift velocity \bar{v}_i . If the material is homogeneous is drift velocity \bar{v}_i directly proportional to intensity of electric field \vec{E} .

$$\bar{v}_i = u_i \vec{E} \quad (23)$$

where u_i is the proportionality constant and is called the mobility of the ion.

If there are N_i ions of species i per unit volume, with charge magnitude of q_i on the i^{th} ion, the ionic conductivity can be expressed as

$$\sigma = \sum_i q_i N_i u_i \quad (24)$$

Stoke's law for the drift of a spherical object in a viscous medium can be used to qualitatively describe the relation between mobility of the ion and the material properties. Sphere with radius r_i embedded in a medium with viscosity η exposure to force $q_i E$

$$u_i = \frac{q_i}{6\pi\eta r_i} \quad (25)$$

In the previous formula, the mobility and thus σ are indirect dependent to viscosity. The quantity $1/\sigma$ called resistivity is consequently nominally proportional to viscosity.

This application of Stoke's law is quite simplified and can be applied only before a curing substance get gelatin. After that it fails completely. The reason is that at gelation process macroscopic molecular network is created and the bulk viscosity became infinite. Nevertheless, the resistivity stays finite because polymer segments which have similar size like the ions are still mobile thanks to diffusion process. The viscosity and ion mobility has similar dependences on mobility of polymer segment.

Effect of conductivity give to increase to a $1/\omega$ frequency dependence in ϵ'' as shown hereinafter

$$\varepsilon'' = \frac{\sigma}{\omega\varepsilon_0} + \varepsilon_d'' \tag{26}$$

where ε_d'' is contribution to ε'' from losses arising from dipolar orientation.

2.5 Dipole orientation

The following figure shows on simplified schematic form influence of electric field to dipole orientation.

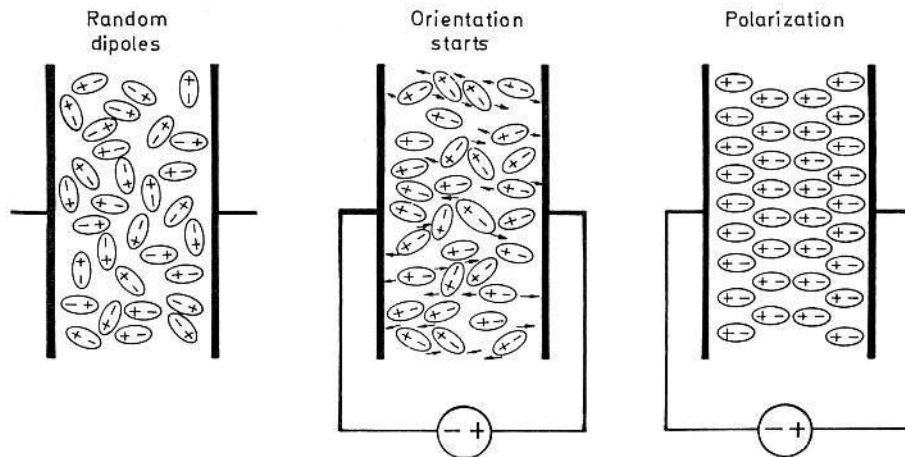


Fig. 5. Schematic illustration of dipole orientation by influencing of electric field [4]

The movement of dipoles in viscous medium is hindered by rising macromolecular network. A typical time is needed for the orientation process. It is so-called dipole relaxation time and mark by τ_d . During a typical cross-linking reaction it grows with going reaction and growing molecular network.

We can use the following distribution for the permittivity:

ε_u the constant permittivity: at the high frequencies the dipoles are not able to follow changes of electric field

ε_r the relaxed permittivity: dipoles are able to follow changes of electric field with minimal relaxation time.

The Debye's model of hindered dipole is the simplest, it supposes one relaxation time for all molecular groups.

$$\varepsilon' = \varepsilon_u + \frac{\varepsilon_r - \varepsilon_u}{1 + (\omega\tau_d)^2} \tag{27}$$

$$\varepsilon'' = \left(\frac{\sigma}{\omega \varepsilon_0} \right) + \frac{(\varepsilon_R - \varepsilon_U) \omega \tau_d}{1 + (\omega \tau_d)^2} \quad (28)$$

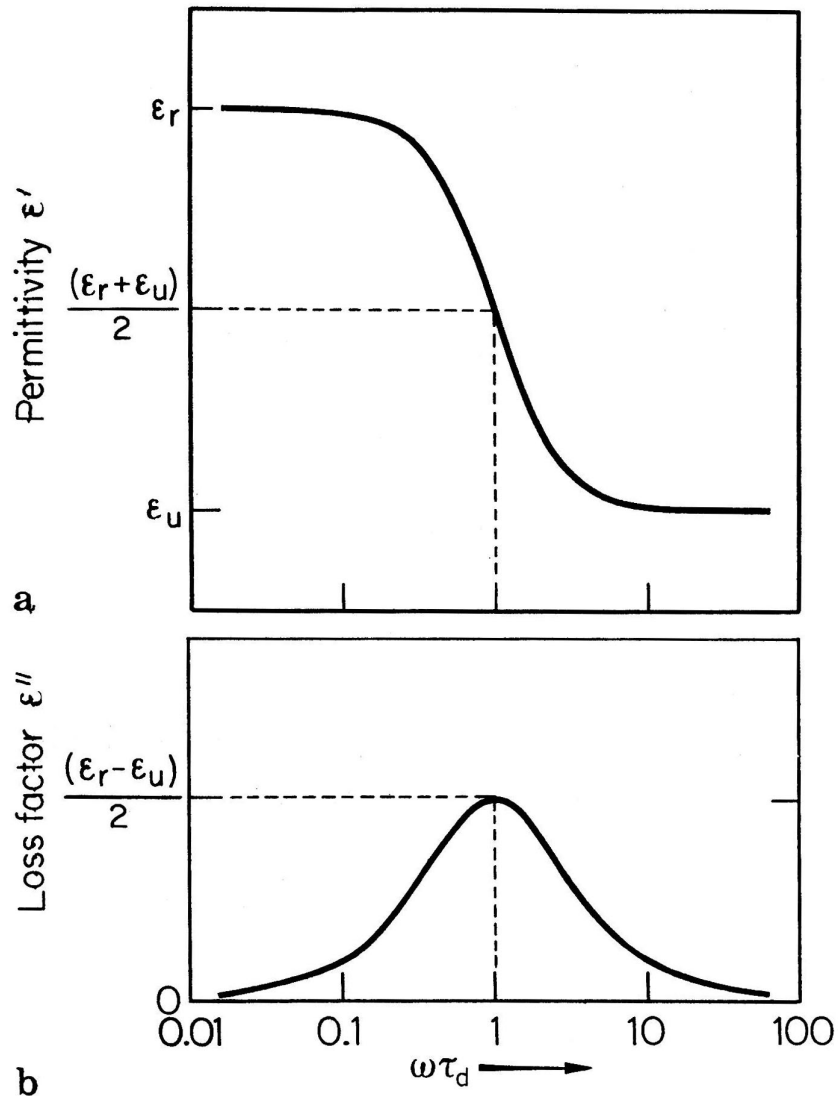


Fig. 6. Debye single relaxation time model for dipole orientation

a) Permittivity b) loss factor [4]

On the figure above is displayed frequency dependence on ε' . From this graph is obvious that ε' is in the middle between ε_u and ε_r if $\omega = 1/\tau_d$. Plot for ε'' shown on Fig. 7 is more complex for the reason that the relative contributions of σ and the dipole loss must be taken into description. On that figure is the simplest case for $\sigma = 0$, $\omega = 1/\tau_d$. If σ has not zero value the dependence $1/\omega$ of ε'' is different from ideal Debye's peak.

Frequency dependences of ε' and ε'' are shown on the Fig. 7 below this plot is known as Cole-Cole diagram. This figure shows idealized case from Fig. 6. When $\sigma = 0$, the Cole-Cole diagram has semicircle shape with intersections in points ε_u and ε_r on the axis x. Maximum value of $\varepsilon'' = (\varepsilon_u - \varepsilon_r)/2$.

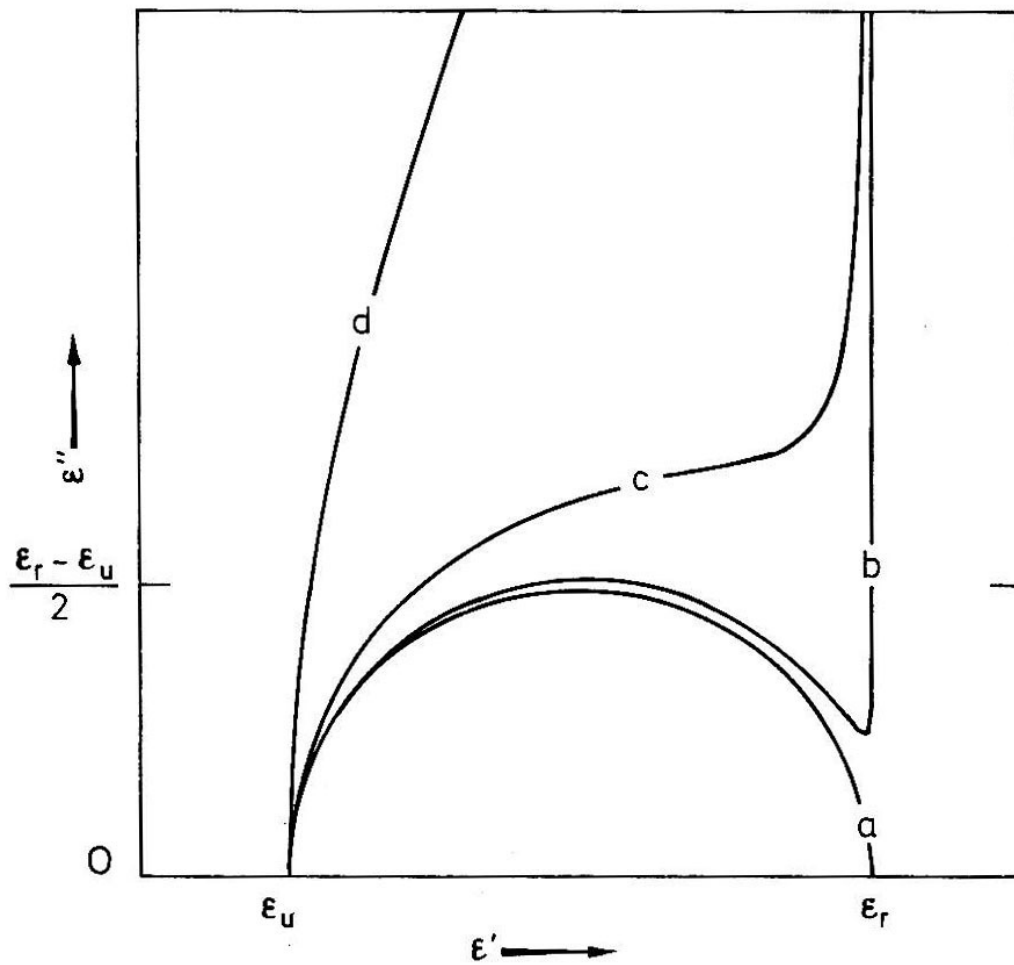


Fig. 7. Cole-Cole diagram showing effect of varying conductivity [4]

3 ULTRAVIOLET-VISIBLE SPECTROSCOPY

Ultraviolet-visible spectroscopy or ultraviolet-visible spectrophotometer (UV/ VIS) is based on visible light and neighboring areas of electromagnetic spectrum. The spectral range used for by spectrophotometers is shown in Fig. 8. Molecules expose to radiation on this wavelengths are undergo electronic transitions.

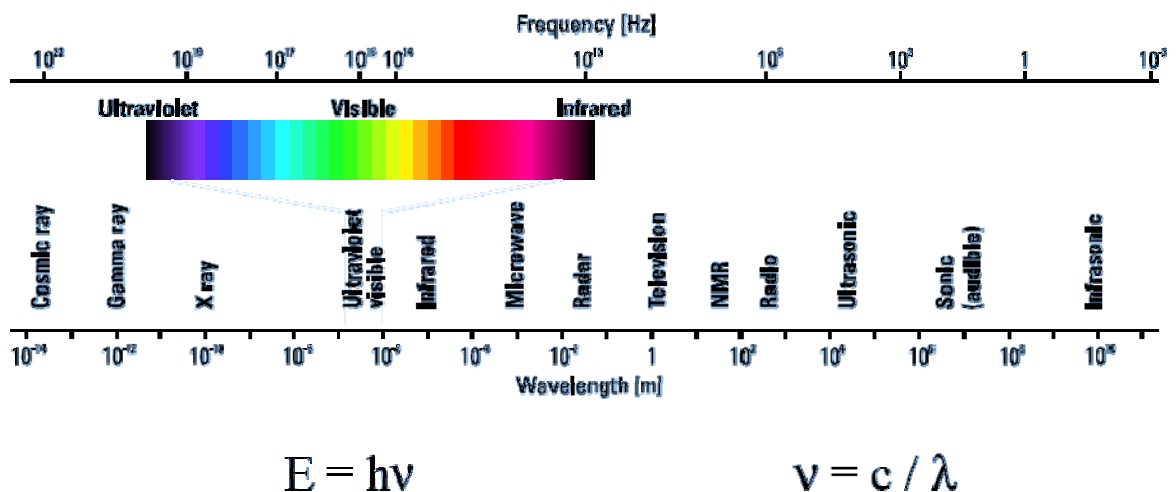


Fig. 8. The Electromagnetic Spectrum [5]

Ultraviolet-visible spectrophotometer

The basic principle is measuring the intensity of light passing through a sample as is displayed on the Fig. 9 The device for this measurement is called spectrophotometer and compares the intensity of light before and after it passes through the sample. This ratio is called transmittance (29) and is articulated as a percentage. Transmittance is used in (30), which express absorbance.

$$\tau = \frac{I_o}{I_l} \quad (29)$$

$$A = -\log\left(\frac{I_o}{I_l}\right) = \frac{I_l}{I_o} \quad (30)$$

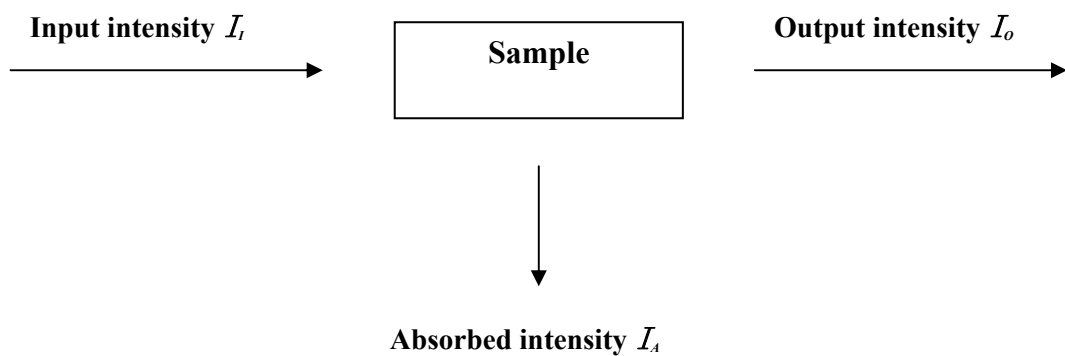


Fig. 9. Scheme of radiant flux through the Sample [6]

Spectrophotometer consist of the light source like an incandescent bulb for the visible wavelengths, or a deuterium arc lamp in the ultraviolet, a holder for the sample, a diffraction grating or monochromator to separate the different wavelengths of light, and a detector. A CCD with diffraction gratings or a photodiode with monochromators are used for the detection. Diffraction gratings gather light of different wavelengths on different pixels. Monochromators are filters which release only single-wavelength light.

Samples are usually placed in the see-through container which is called cuvette. It is usually rectangular cell made of plastic or glass. The best are made of quartz.

There are two types of spectrophotometers - single beam or double beam. Device with Single beam is older type. It uses only one ray which passes through the sample and for the measuring of total intensity the sample has to be removed. Basic principle is illustrated in Fig. 10

Device with double beam uses also one source of light but before it passes thorough the sample one ray of light is split into two. One goes through it and the second is used for reference. Some devices based on this principle have two detectors and the both intensity are measured in one time.

Other instruments uses so-called beam chopper, which release only one beam at a time thus only one detector is needed. Schematic view is displayed in Fig. 11.

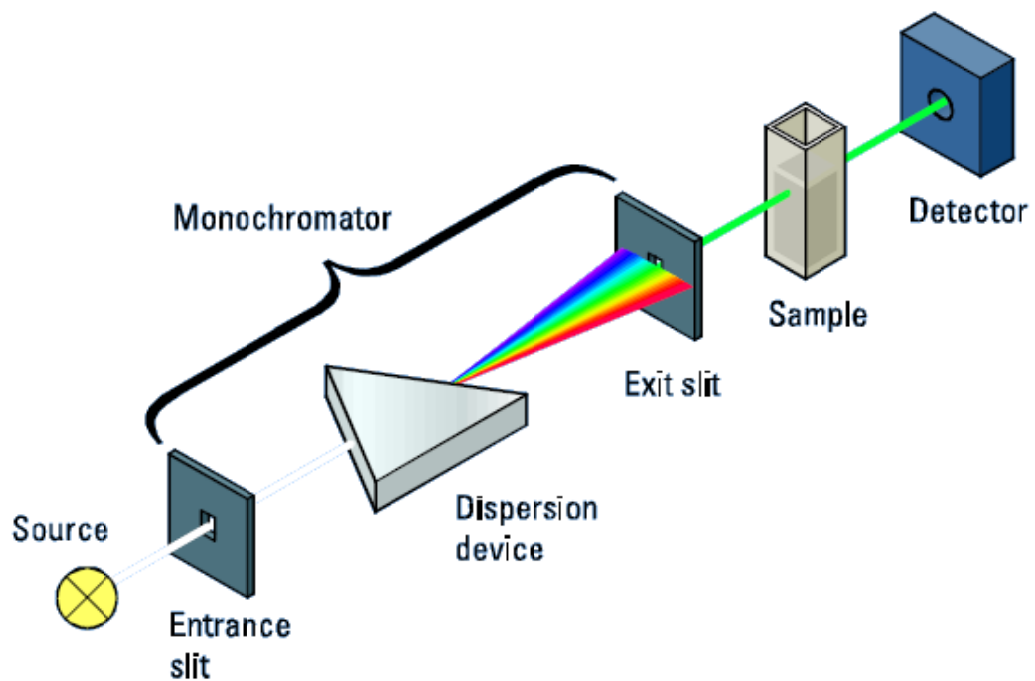


Fig. 10. Schematic of a conventional single-beam spectrophotometer [5]

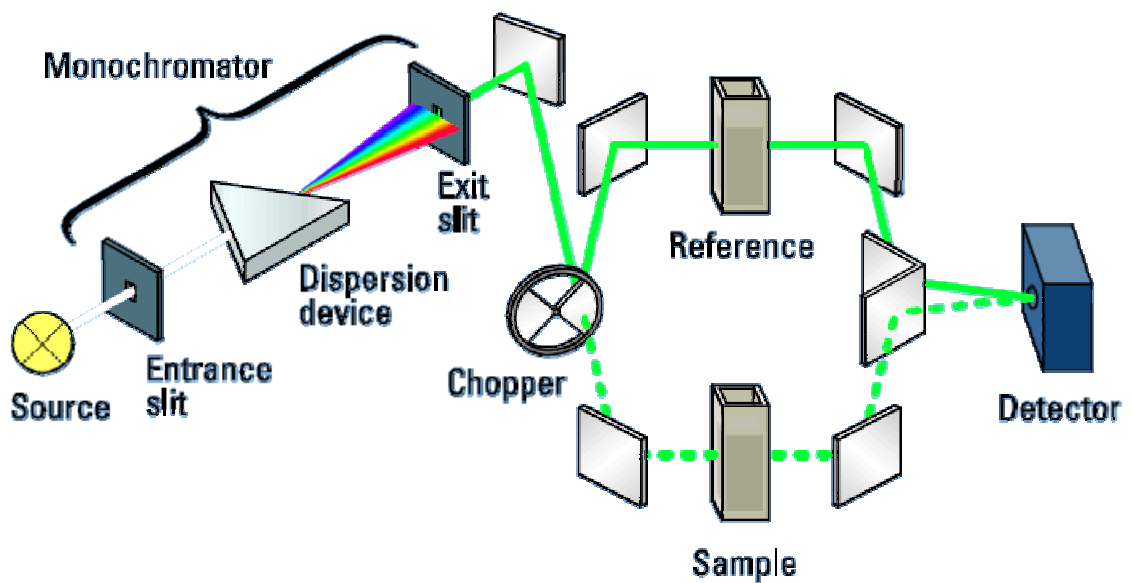


Fig. 11. Optical system of a double-beam spectrophotometer [5]

For quantitative identification of compounds is used absorption spectrum. It is dependence of absorbance on wavelength or frequency. Absorbance at specific wavelength depends on concentration and thickness of layer according Lambert-Beer law:

$$A_{\lambda} = \varepsilon_{\lambda}bc \quad (31)$$

where A_{λ} is absorbance at wavelength λ , ε_{λ} is molar absorption coefficient at wavelength λ , b is thickness of layer and c is concentration.

II. ANALYSIS

4 HARDWARE

4.1 Hewlett Packard 4284A Precision LCR Meter

The HP / Agilent 4284A Precision LCR Meter is a cost-effective solution for component and material measurement. The 4284A may be used to improve component quality by providing an accurate, high-throughput test solution. The wide 20 Hz to 1 MHz test frequency range and superior test-signal performance allow the 4284A to test components to most commonly referenced test standards, such as IEC/MIL standards, and under conditions that simulate the intended application. Whether in research and development, production, quality assurance, or incoming inspection, the 4284A will meet all of your LCR meter test and measurement requirements. [10]



Fig. 12. The HP 4284A Precision LCR Meter

4.2 Technological card NI-488.2

IEEE-488 is a short-range, digital communications bus specification. It was originally created for use with automated test equipment, and is still in wide use for that purpose. IEEE-488 is also commonly known as HP-IB (Hewlett-Packard Instrument Bus) and GPIB (General Purpose Interface Bus). It allows up to 15 devices to share a single 8-bit parallel electrical bus by daisy chaining connections. The slowest device participates in control and data transfer handshakes to determine the speed of the transaction. The maximum data rate

is about one Mbyte/sec in the original standard, and about 8 Mbyte/sec with IEEE-488. The IEEE-488 bus employs 16 signal lines — eight bi-directional used for data transfer, three for handshake, and five for bus management — plus eight ground return lines.

4.3 Memmert Universal oven Model UNP 200

- natural convection
- adjustment of pre-heated fresh air admixture by air flap through process controller in 10% steps for each segment individually
- vent connection with restrictor flap
- adaptive, fuzzy-supported, multifunctional, digital microprocessor PID-controller
- autodiagnostic system with fault indication
- 2 Pt100 sensors Class A in 4-wire-circuit, mutually monitoring and taking over the performance at the same temperature value
- digital 7-day-programme-timer with real time clock, precise minute setting, for one set value or start of ramp operation
- digital display (LED) of all set parameters, such as temperature, weekdays, time, air flap position, programme status and set-up values
- resolution of display for set value 0,1 °C below 99,9 °C, 0,5 °C above 100 °C; for actual value 0,1 °C
- long-term logging (ring store) of all relevant data, GLP-conforming as data logger - 1024 kB
- programme stored on power failure
- parallel printer interface (incl. real-time clock with date function) for all PCL3-compatible ink-jet printers for GLP-conforming documentation
- serial interface RS 232 including MEMMERT Software "Celsius 2007" for programming and documentation

- chip card control incl. one MEMoryCard XL with 32 kB (up to 40 ramps)
- incl. works calibration certificate for +160 °C [11]

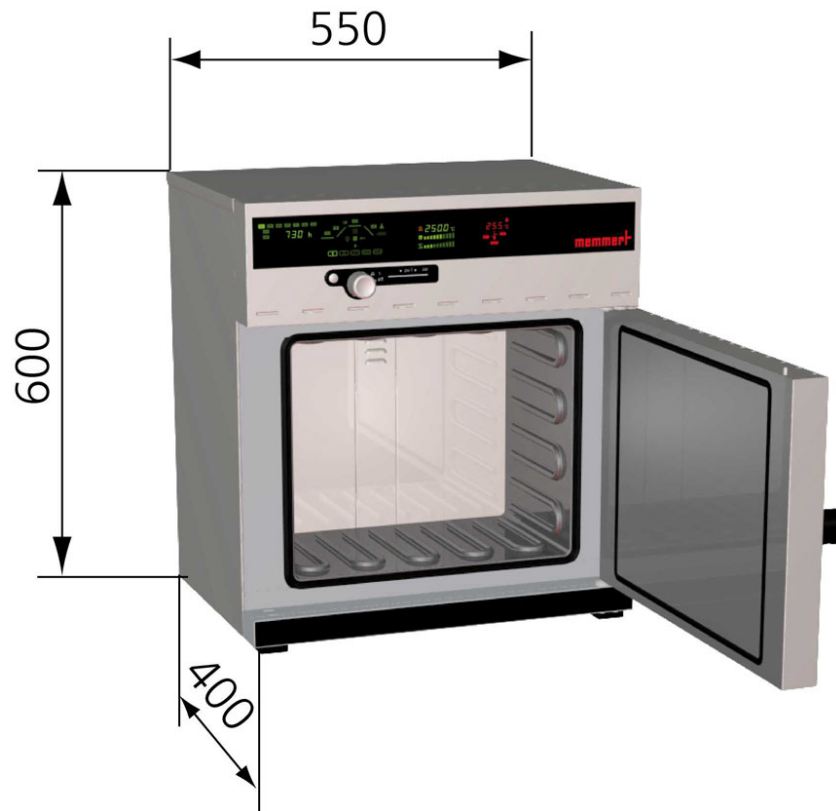


Fig. 13. Memmert Universal oven Model UNP 200 [11]

4.4 Helios Alpha spectrophotometer

The Helios Alpha spectrophotometer is ideal for busy industrial and research labs that value productivity, durability, and the ability to perform a wide range of UV-Visible analyses.

The Helios Alpha is a high-energy double-beam system with the software, sample handling, and the data handling versatility to improve your lab's productivity and efficiency.

The Helios Alpha has many benefits built-in:

- floppy disk & internal memory for reliable test/data storage
- password-protected logon with administrator-defined user rights
- thermostatted 7-cell changer for automatic multiple sample measurement
- export data to LIMS via RS232



Fig. 14. The Helios Alpha spectrophotometer

5 SOFTWARE

5.1 Agilent VEE 8.0

Agilent VEE is a Visual Engineering Environment that allows you to program by creating intuitive “block diagrams.” You select and edit objects from pull-down menus and connect them to each other by wires to specify the program’s flow, mimicking the order of tasks you want to perform. Users can quickly create, test, and update code because programs can be run and debugged on the fly by using Agilent VEE’s Start, Stop, and Pause buttons, as well as Watch Window debugging feature. Programs are also self-documenting. Agilent VEE illustrates the connections between individual objects, so programs are easily understood by others. With the help of Code Completion and Code Insight, users can create programs easier and faster. Plus, with Agilent VEE’s built-in tutorials and numerous sample programs, demos and context-sensitive help, beginners and veteran programmers alike can get started quickly and stay productive.

6 MEASURING WORKSPACE AND ITS PREPARATION

The main used measuring device is LCR meter HP4284A which is interconnected with personal computer via GPIB as is shown in Fig. 15. The process of measuring is controlled by program written in Agilent VEE Pro 8.0. The program is named *3f-dissipation.vee* and it is based on program created by Milan Navrátil in [1]. The modification has been made with author's permission. This program is described in 6.1

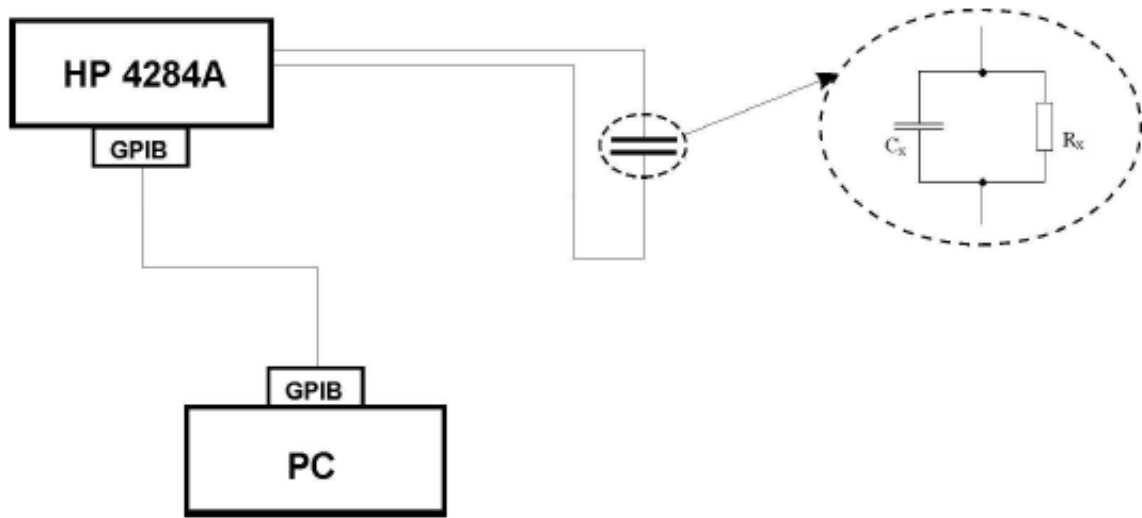


Fig. 15. Scheme of measuring chain [1]

6.1 User applications in VEE pro

6.1.1 Application for measuring of dissipation factor

This program was created because writing of data from LRC meter manually is almost impossible and definitely impossible if the data has to be written for example every second. This task could not be done manually. Automated acquisition system is needed. VEE Pro 8.0 was chosen for this task. This graphically oriented language is very efficient for these types of jobs.

This application is designed for measuring of dissipation factor at three frequencies. These frequencies can be changed by user in text fields labeled Freq 1, Freq 2, and Freq3. Used LCR meter can set frequency in range from 20 Hz to 1 MHz. So user can input any frequency from this range. But frequency generated by LCR meter can be little bit different from given because internal generator is not able to create all frequencies exactly due to its limitation. This application can be seen in the Fig. 16 and Fig. 17

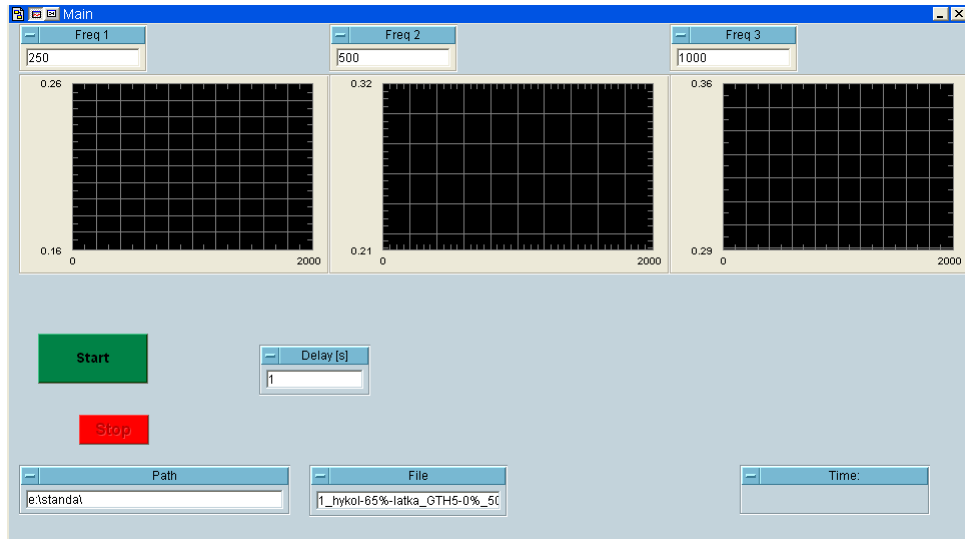


Fig. 16. The appearance of the user application screen used for measurement of the dissipation factor created in Agilent VEE Pro.

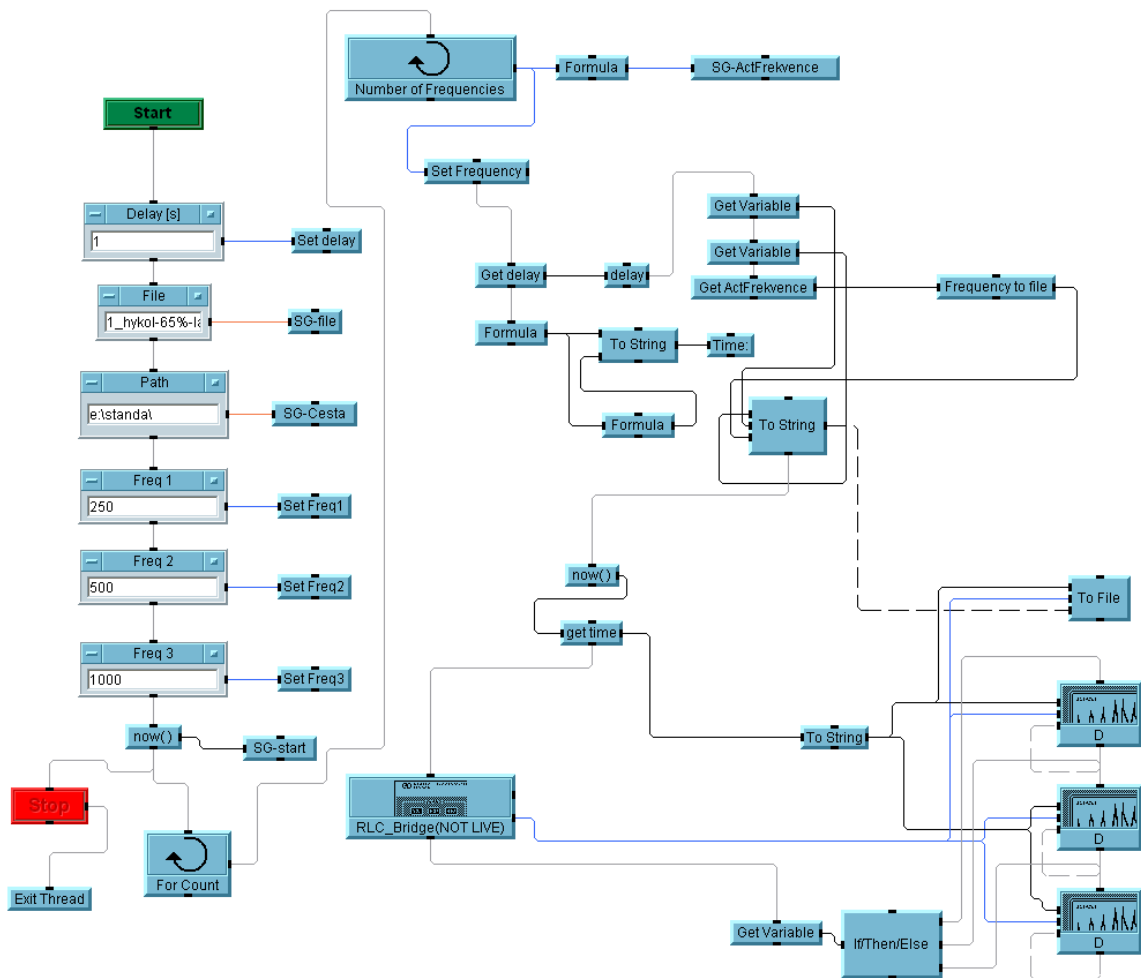


Fig. 17. Graphic “source code” of program for measuring dissipation factor created in Agilent VEE Pro.

The user screen shown on Fig. 16 has three plots for displaying values of dissipation factor in time. Also there are some input text fields. Three of them are labeled: “Freq 1”, “Freq 2” and “Freq 3”. They are for frequencies setting. Next, named “Delay” is for setting of delay between each reading of dissipation factor from the LCR meter. The purpose of rest two fields is obvious. The field named “Path” is for setting directory for saving obtained data and “File” is the name of which will be used for file with data.

The application is launched by green button “Start” and is finished by red button “Stop”. The time which has flown since the Start button has been pressed is displayed in the field called “Time”.

After pressing Start button the global variables are set. The “body” of program is created by two cycles. One of them during its run is reading dissipation factor for all given frequencies and also saving to files is done here. The purpose of second of them is to procure repeating of the first cycle.

Received data is being saved to the three text files according to frequency. Files are distinguished automatically by adding numerical value of frequency to the relevant file.

6.1.2 Application for quick displaying saved data

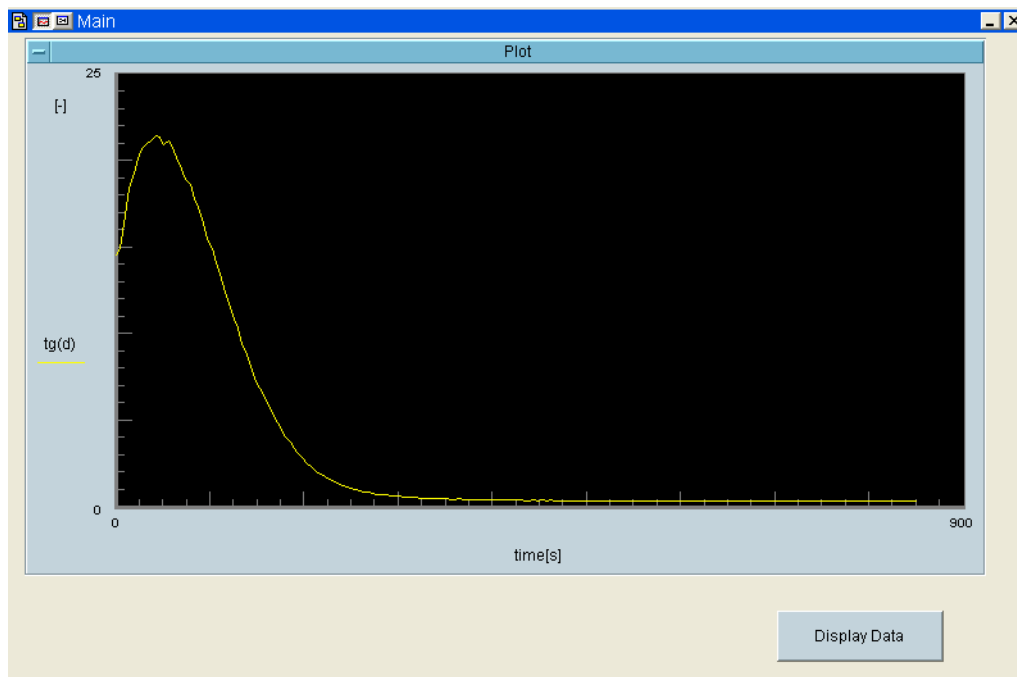


Fig. 18. The appearance of the user application screen used for displaying of the dissipation factor from the saved file created in Agilent VEE Pro.

With growing amount of saved files with data emerged need for fast displaying of those data. Spreadsheet program like Excel looked suitable for this but although it is not difficult to do this job with it, there is better solution. The application only for this purpose was created. Their advantage is that, there is only one button and plot nothing more. User interface is shown in Fig. 18. After the button “Display Data” is pressed, the file name selection window will pop-up and user can choose right file to display.

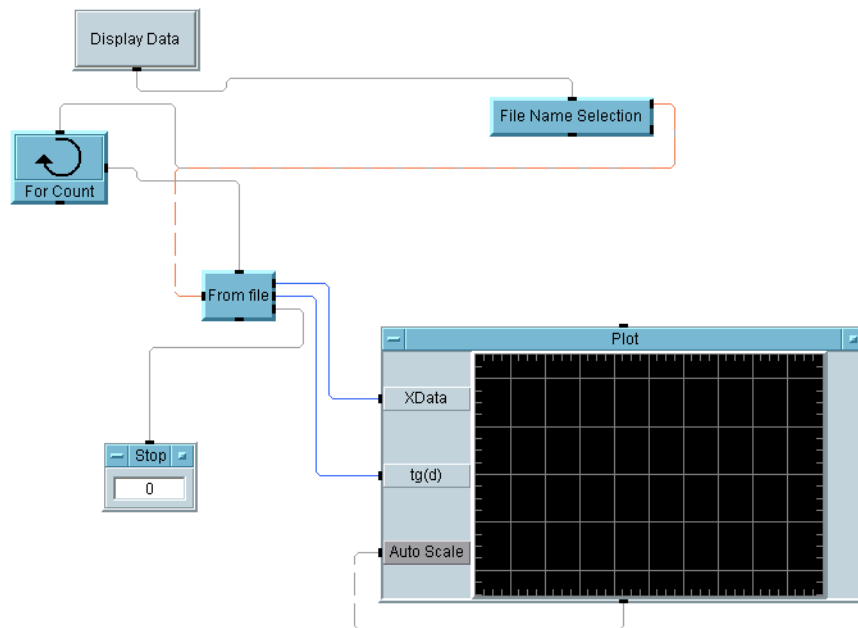


Fig. 19. Graphic “source code” of program for used for displaying of the dissipation factor from the saved file created in Agilent VEE Pro.

6.2 Dielectric spectroscopy method

Dissipation factor have been chosen because is not dependent on distance between electrodes and its surface. It depends on angular frequency which remains constant, on permittivity and conductivity of material. Change of permittivity is caused by falling quantity of dipoles. Cross-linking reaction also has an impact on conductivity.

Steel electrodes shown on Fig. 20 have been used for practical realization. To prevent their pollution by tested sample have been covered by aluminum foil on the side of contact with a sample. This solution also helps with weighing of sample because sample placed on the

foil could have been weighing only with it not with much more heavier steel electrode which was overweight for our balance. A piece of plastics with “U” shape have been put between electrodes like a spacer. Its purpose was to avoid short-circuit.



Fig. 20. Measuring electrodes covered by aluminum foil + plastic spacer

6.2.1 Epoxy resin

Cross-linking reactions of epoxy resins are quite well described so this is the reason why they have been chosen to verify used method.

Measuring was done at three frequencies 250 Hz, 500 Hz and 1000 Hz which have been changing in the loop during the measuring. It was repeated several times. This measurement was repeated at different temperatures (at 22°C, 30°C, 40°C and 50°C) to probe influence of temperature. Obtained data has been processed in Matlab. Because we were not interested in absolute value of dissipation factor, only in its maximum value in time, simple modification has been done. All measured data has been transformed into 0 to 1 range. So dependence of dissipation factor on time could be easily compared.

This modification is done:

$$\frac{D_0 - \min(D_0)}{\max(D_0 - \min(D_0))} \quad (32)$$

Where, D_0 is set of raw data

Chosen data after this modification is displayed below. Rest can be found in appendices.

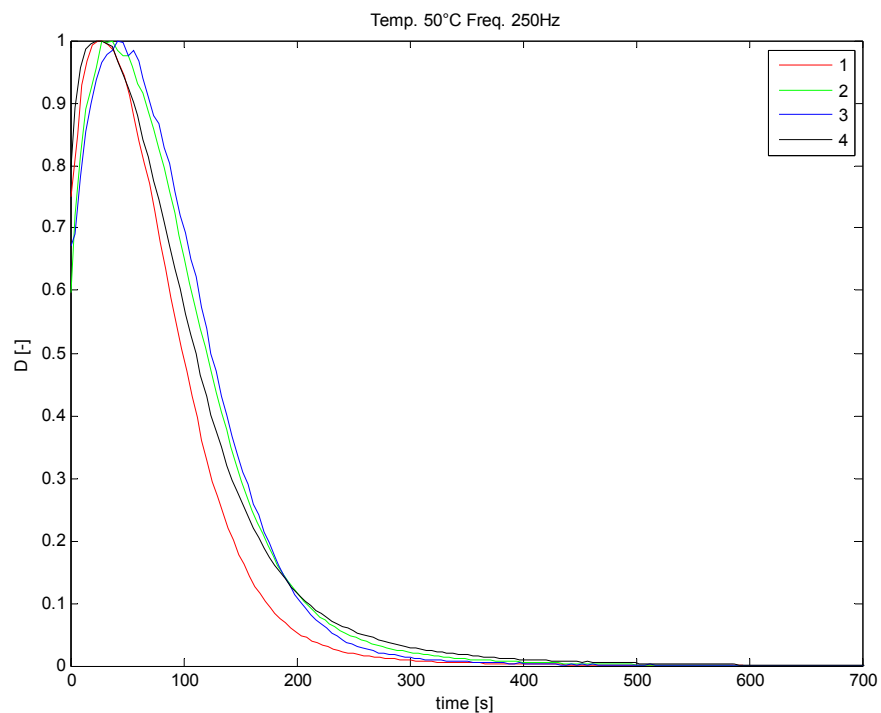
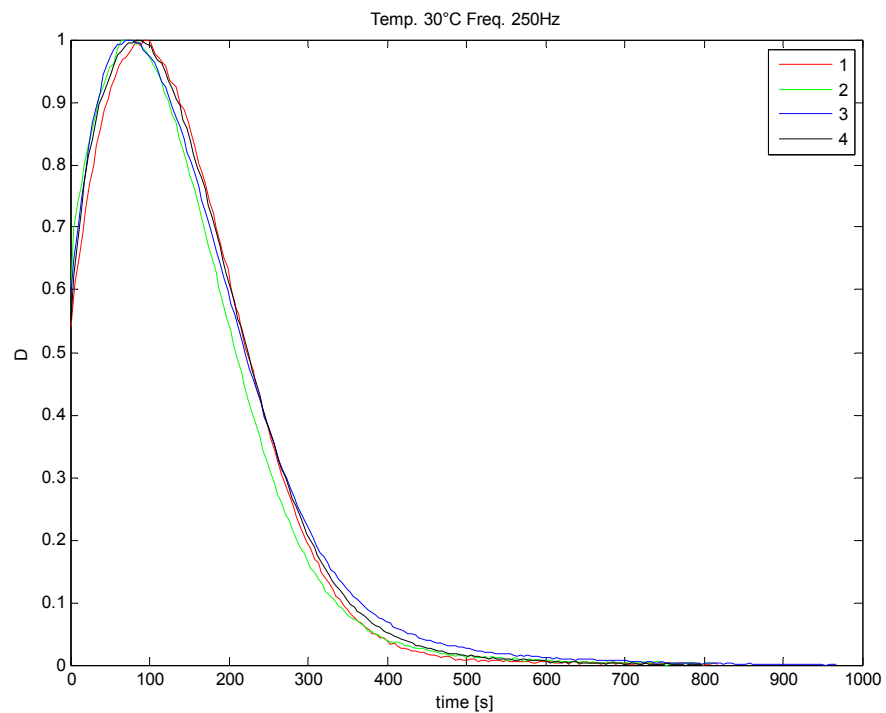


Fig. 21. Time dependence of dissipation factor during the cross-linking reaction at 30°C and 50°C for 250 Hz. Both plots show four measurements which are labeled 1,2,3,4.

	Frequency [Hz]		
	250	500	1000
Temperature [°C]	Time [s]		
22	139.2	123.5	111.2
30	84.2	74.4	65.6
40	45.4	37.8	34.8
50	29.1	33.1	30.0

Table 3 Time dependence of cross-linking
on temperature and the frequency

The Table 3 shows the dependence of speed of cross-linking reaction on temperature and frequency. Data in this table is averages from all four measurements. It can be told that reaction is getting faster with rising temperature. Also position of the peak is dependent on frequency. The higher frequency the earliest peak formation is observed. Only for 50°C is situation different but the differences are minor.

6.2.2 Hykol

At first solution from powdered hykol and distilled water was prepared. hykol in powder was dissolved in water so that spare 56% aqueous solution of hykol was prepared. Concentration has experimentally obtained in [1]. Solution was prepared in the plastic bottle. There was also stored. Solution was not ready to use immediately because it was full of air after mixing. Some relaxing time was needed. Secondly, the sample was placed on aluminum foil and 0.5 g of hykol was weighed. And at last the sample on the aluminum foil was put on electrode as is shown in Fig. 20 and a certain amount of the cross-linking agent (25% aqueous solution of glutaraldehyde) added from micropipette. Then the sample was mixed by plastic stick and second electrode was put on.

For data gathering was used program written in VEE Pro and described in 6.1. It was the same program which had been used for epoxy measuring. Obtained dependence can be seen in the following figure.

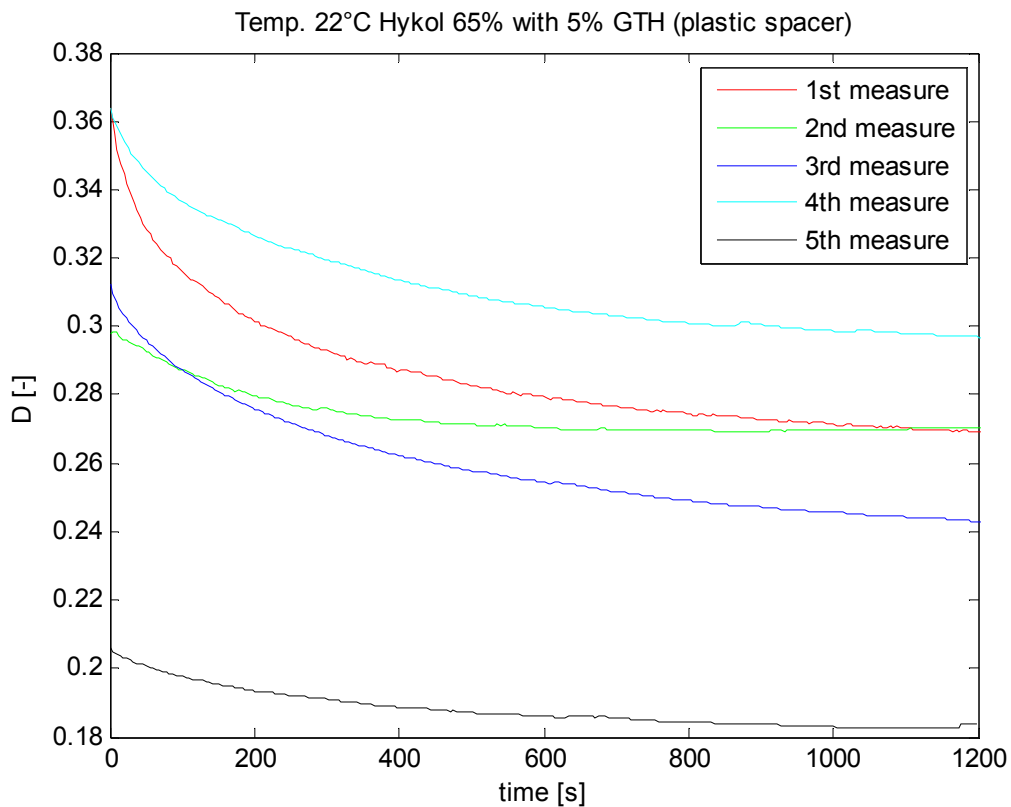


Fig. 22 Sample (Hykol with 5% b.w. of glutaraldehyde), five same measurements at 250 Hz

Data displayed on Fig. 22 has not been standardized yet because the difference between starting and ending value of dissipation factor was too small as can be seen above.

It was a reasonable assumption that the solution with hykol contains too much water and thus measuring had been negatively influenced by this fact.

For elimination of this impact the concentration of aqueous solution of hykol was changed from 56% to 65%. Also plastic spacer was removed and substituted by cotton fabric. Now the sample was not placed directly on the aluminum foil but it was placed on the fabric as shown in the Fig. 23. The textile was used because it can absorb water and thus it can contribute to lower amount of water in the sample.

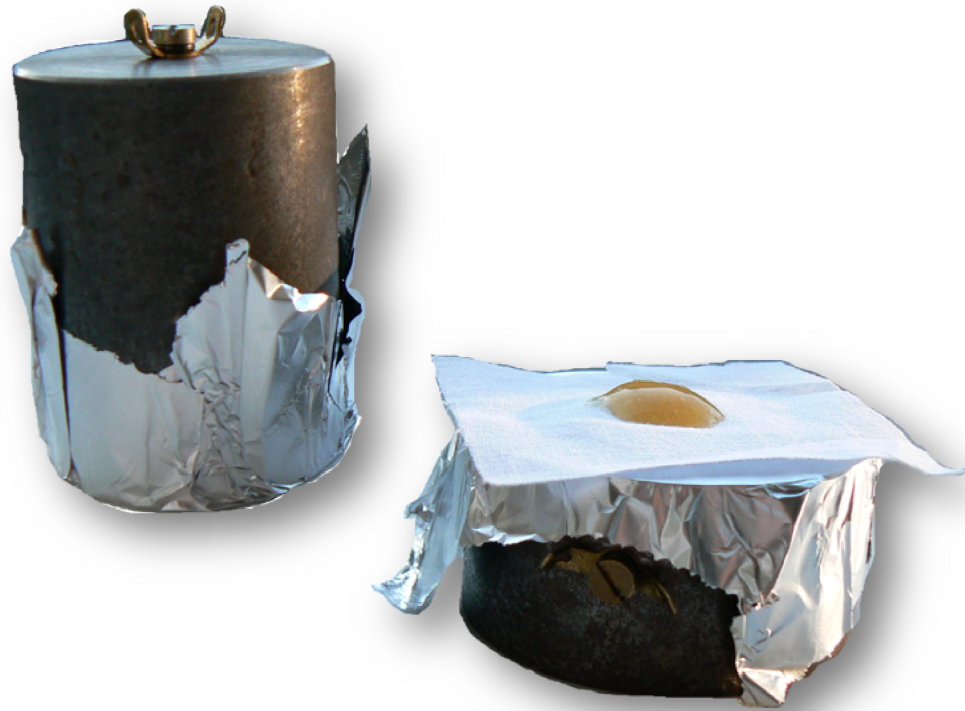


Fig. 23. Measuring electrodes covered by aluminum foil + sample on the fabric.

Nevertheless, it did not help. Obtained characteristic looked differently from our expectation. Differences between beginning and ending remain almost unchanged in all cases.

Thus the blind test (only hykol was placed between electrodes) has been performed. Its results were similar to normal test where hykol was cross-linked by agent (GTH). The results are displayed in the Fig. 24. As can be seen in the Table 4, the fall of dissipation factor is bigger in case of hykol + %5 GTH only at 1 kHz is situation different. But we cannot say that these differences are big enough so as we could say that we do not measure only noise. Also we found out that if hykol is cross-linked by GTH it looks fully cross-linked after 80 seconds. That was find out only by visual observing so it is not exact data but at any rate there is no peak at the most cases. More measurement for various temperatures have been done, they can be found in the appendix C.

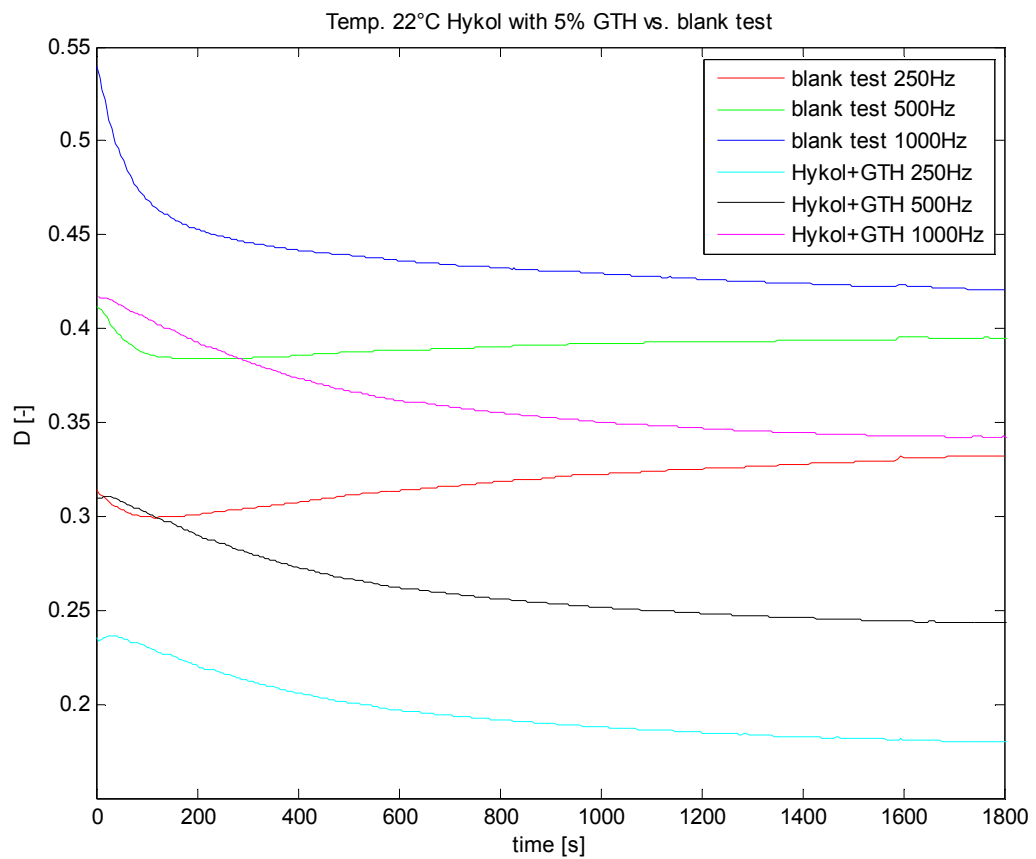


Fig. 24. Blank test (only hykol) and cross-linking at 22°C, for frequencies 250Hz, 500Hz and 1 kHz

Frequency [Hz]	Blank test	Hykol+5%GTH
250	0.0186	0.0551
500	0.0168	0.0668
1000	0.1193	0.1073

Table 4. Absolute values of drop of dissipation factor

7 SPECTROPHOTOMETRIC MEASUREMENT OF ABSORBANCE

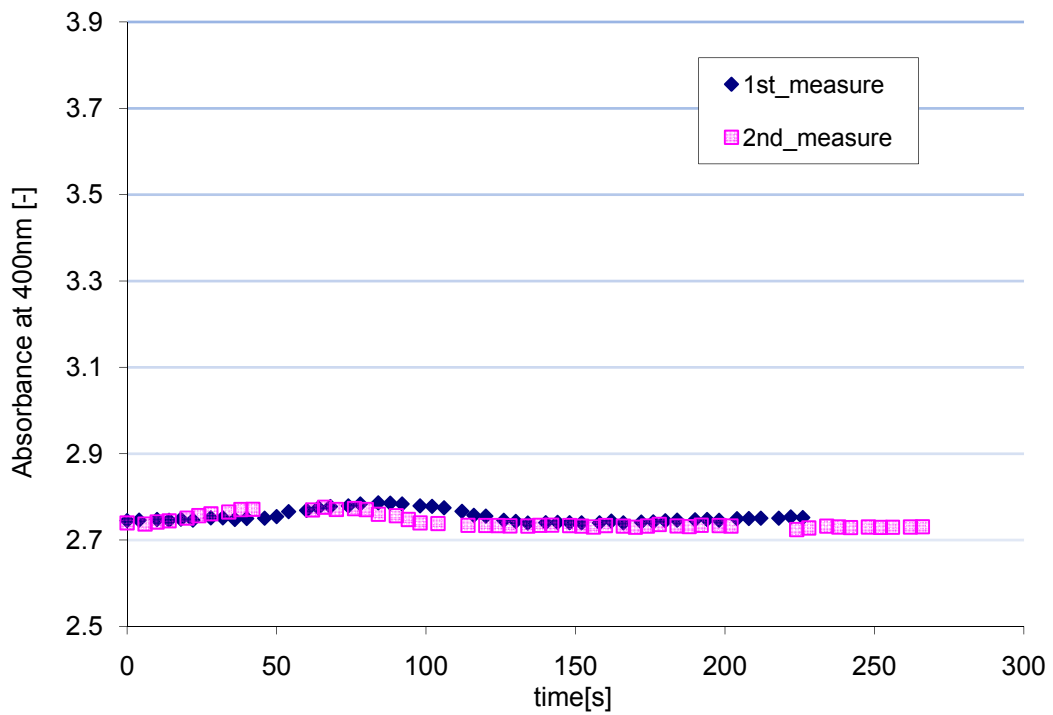


Fig. 25. Absorbance blank test

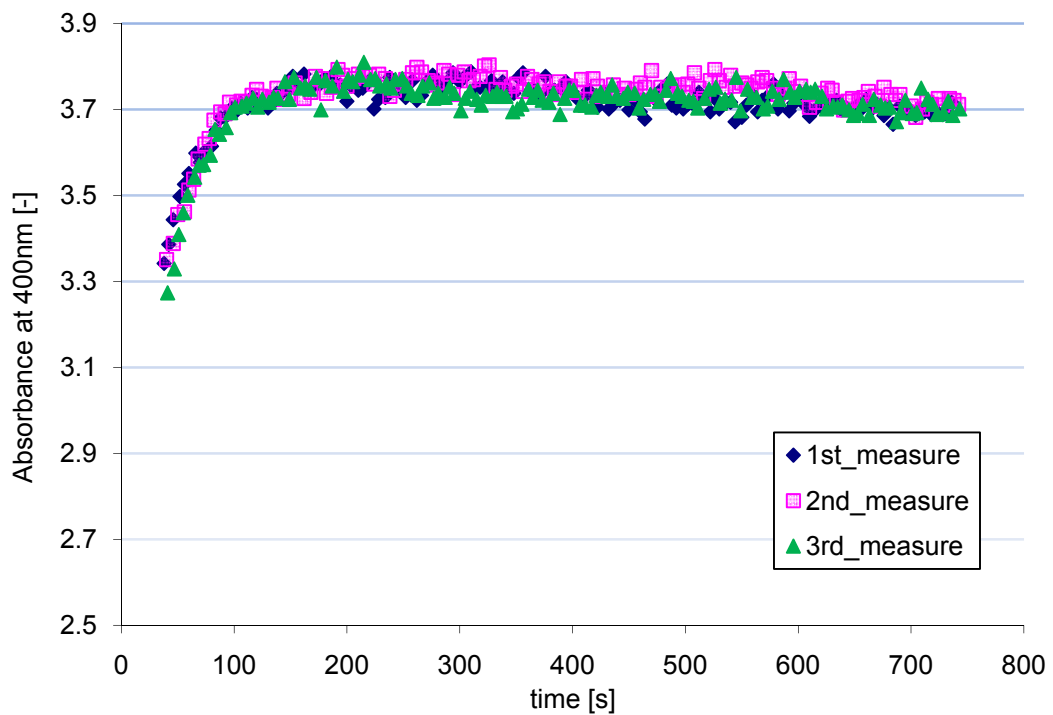


Fig. 26. Absorbance hykol + 6% GTH

Although usage of this measuring method was not mentioned in the assignment, it was decided to add it. Helios Alpha UV-Vis spectrophotometer has been used. It is not bad device but even though is equipped by RS-232, the communication with pc via this interface appeared impossible due to unknown list of commands. This device can communicate with PC via RS-232 on condition that commercial software is used. But this software is quite expensive and it was not available. Next possibility how to get data was obsolete 3.5" FDD. So the data was saved to diskette in csv format and transferred into PC where it has been processed.

Two different measurements were performed. Measuring of absorbance has been done at 400nm for all measurements.

In the first case there was only hykol in the cuvette. Two same measurements have been done; the data from both measurements is displayed in the Fig. 25. As can be seen absorbance approximately remains in the interval from 2.7 to 2.8. Exact average data is displayed in the Table 5.

In the second case the hykol was cross-linked by glutaraldehyde. The absorbance has changed to 3.7. Average values from all three measurements can be found in Table 6. These values have been obtained from steady state which beginning at 100 s c. But it has been decided to take into account values after 150 s since the start of reaction. It has been done to assure that values included into calculation are really the values of steady state.

So absorbance has changed from 2.7482 to 3.7196 after reaction. This process took according to Fig. 26 about 100 s.

n	Average Absorbance	Standard deviation	min.	max.
1	2.7546	0.0143	2.7393	2.7860
2	2.7418	0.0150	2.7240	2.7760
1+2	2.7482	0.0160	2.7240	2.7860

Table 5. Average absorbance of hykol

n	Average Absorbance	Standard deviation	min.	max.
1	3.7292	0.0288	3.6656	3.7878
2	3.7513	0.0246	3.6819	3.8041
3	3.7306	0.0258	3.6716	3.8097
1+2+3	3.7196	0.0684	3.2732	3.8097

Table 6. Average absorbance of cross-linked hykol

(After 150s since the start of reaction)

CONCLUSION

The current measuring workplace has been improved with wires used for connection of electrodes to LCR meter. They were extended with cable containing silicon isolation because we need longer cables and also we demand higher temperature heat stability of isolation due to measurement in the oven.

The program for real-time measuring of dissipation factor has been created in Agilent VEE PRO. This program allows measuring dissipation factor at three user-settable frequencies which are changing in the loop during the measurement. The purpose of this program is reading of data from LCR meter and to save it into text files for the next processing.

At first, the test with epoxy resin has been accomplished. Its purpose was to check eligibility of dielectric spectroscopy for testing cross-linking reactions. Epoxy resins are described very well in the literature and thus they have been chosen for proving usability of this method. The first measure was done at 22°C for three frequencies (250 Hz, 500 Hz and 1 kHz) during one measurement. This measurement was repeated four times. We repeated the same measurement at temperatures 30°C, 40°C and 50°C in the oven. The results can be found in the Appendix A. But for easier comparison of these data the standardization by equal (32) has been done.

According to results of measurements in chapter 6.1.1 it can be told that this reaction is temperature dependent and with growing temperature the peak of dissipation factor is moving to the left on the time axis. Also higher frequencies have the same effect.

The dielectric spectroscopy method has been found suitable for researching kinetics of cross-linking reactions.

We expected similar results for measuring of cross-linking reaction of hydrolyzed collagen with GTH because we used the same technique. Nevertheless, although the results with epoxy resin were perfect, for hykol they were not. It was surprise because we expected similar results as described in [1] where the author has nice results with dielectric spectroscopy used for testing hykol. Almost all measurements of hykol looked like some noise only. We blamed high amount of water in the sample on that. The new solution with less amount of water has been prepared from hykol. We prepared 65% aqueous solution from hykol (previously used was 56%). Also we replaced plastic spacer by cotton fabric which has ability to absorb water. We repeated measure. The results remained almost the same. If

they were compared with blank test they still looked like noise there was only little improvement.

Nevertheless, we have repeated this measure for various temperatures because it has to be done to meet demands given in assignment.

Dielectric spectroscopy has been found unsuitable for testing cross-linking of hydrolyzed collagen by glutaraldehyde. It was due to high volume of water in the tested sample.

Moreover, we used a spectrophotometry method because the change in colour can be observed during the reaction. It was found out that absorbance has changed from 2.74 to 3.72 during approximately 100 s.

All given task have been completed and one extra has been added. However, we did not achieve the same results with dielectric spectroscopy for testing cross-linking hykol by glutaraldehyde like in previous works [1], [9]. The most probable cause was high amount of water in the tested sample. We tried to do some steps to improve it but without significant results. For the future research, we suggest to decrease volume of water in the tested sample or use another method for testing.

BIBLIOGRAPHY

- [1] Navrátil, Milan: Instrumentace a zpracování signálů při měření kinetiky síťovacích reakcí pomocí impedanční spektroskopie, Diplomová práce, UTB Zlín 2002
- [2] Hedvig, Péter: Dielectric spectroscopy of polymers, Akadémiai Kiadó Budapest 1977
- [3] Collagen [cit. 2008-16-05]. Accessible on WWW:
<http://en.wikipedia.org/wiki/Collagen>
- [4] Epoxy Resins and Composites IV, Akademie-Verlag Berlin 1987
- [5] Fundamentals of modern UV-visible spectroscopy, 00000209.PDF, Accessible on WWW: www.hp.com
- [6] Navrátil, Milan: INSTRUMENTATION AND DIAGNOSTICS OF POLYMER COMPOSITES, Doctoral Thesis, UTB Zlín 2007
- [7] Glutaraldehyde [cit. 2008-16-05]. Accessible on WWW:
<http://en.wikipedia.org/wiki/Glutaraldehyde>
- [8] Stanislav Ďaďo, Marcel Kreidl: Senzory a měřicí obvody, Vydavatelství ČVUT, Praha 1996
- [9] Fraden Jacob: Handbook of Modern Sensors: Physics, Designs, and Applications, 2nd ed. New York, Springer Verlag, 1996
- [10] Agilent 4284A Precision LCR Meter [cit. 2008-16-05], 4284a.pdf, Accessible on WWW: <ftp://ftp.testequity.com/pdf/4284a.pdf>
- [11] Universal oven Model UNP 200 [cit. 2008-16-05], Accessible on WWW:
http://www.memmert.com/en/products/product-range/universal-ovens/models/model/UNP_200-4/

LIST OF ABBREVIATIONS

GTH		Glutaraldehyde
i	[A]	Electric current
u	[V]	Electric voltage
t	[s]	Time
τ_d	[s]	Relaxing time
φ	[rad]	Phase difference
ω	[rad.s ⁻¹]	Angular frequency
f	[Hz]	Frequency
A	[-]	Absorbance
A_λ	[-]	Absorbance at wavelength λ
I_A	[W]	Absorbed radiant flux
I_I	[W]	Input radiant flux
I_o	[W]	Output radiant flux
λ	[m]	Wavelength
R	[Ω]	Electric resistance
C	[F]	Electric capacity
S	[m ²]	Area of electrodes
l	[m]	Distance between electrodes
ε^*	[F.m ⁻¹]	Complex dielectric function
ε_0		Dielectric permittivity of vacuum
R_x	[Ω]	equivalent parallel resistance
C_x	[F]	equivalent parallel capacity
σ	[S.m ⁻¹]	Electric conductivity
ρ	[$\Omega.m$]	Static resistivity

D	[-]	dissipation factor
$\text{tg } \delta_x$	[-]	dissipation factor
\vec{E}	[V.m ⁻¹]	electric field strength
ε_λ	[m ² mol ⁻¹]	molar absorption coefficient at wavelength λ
c	[mol.m ⁻³]	concentration
ε_d''	[F.m ⁻¹]	contribution to ε''
ε''	[F.m ⁻¹]	imaginary part of the complex dielectric function

LIST OF FIGURES

Fig. 1. Apparatus applies a time-varying voltage $u(t)$ to the electrodes and measures the time varying current $i(t)$ [4].....	13
Fig. 2. Sinusoidal voltage and current waveforms having a phase difference ϕ	14
Fig. 3. Equivalent circuit for the admittance	15
Fig. 4. Impedance in the complex plane	16
Fig. 5. Schematic illustration of dipole orientation by influencing	19
Fig. 6. Debye single relaxation time model for dipole orientation.....	20
Fig. 7. Cole-Cole diagram showing effect of varying conductivity [4].....	21
Fig. 8. The Electromagnetic Spectrum [5].....	22
Fig. 9. Scheme of radiant flux through the Sample [6].....	23
Fig. 10. Schematic of a conventional single-beam spectrophotometer [5].....	24
Fig. 11. Optical system of a double-beam spectrophotometer [5].....	24
Fig. 12. The HP 4284A Precision LCR Meter.....	27
Fig. 13. Memmert Universal oven Model UNP 200 [11].....	29
Fig. 14. The Helios Alpha spectrophotometer	30
Fig. 15. Scheme of measuring chain [1]	32
Fig. 16. The appearance of the user application screen used for measurement of the dissipation factor created in Agilent VEE Pro.	33
Fig. 17. Graphic “source code” of program for measuring dissipation factor created in Agilent VEE Pro.....	33
Fig. 18. The appearance of the user application screen used for displaying of the dissipation factor from the saved file created in Agilent VEE Pro.	34
Fig. 19. Graphic “source code” of program for used for displaying of the dissipation factor from the saved file created in Agilent VEE Pro.....	35
Fig. 20. Measuring electrodes covered by aluminum foil + plastic spacer	36
Fig. 21. Time dependence of dissipation factor during the cross-linking reaction at 30°C and 50°C for 250 Hz. Both plots show four measurements which are labeled 1,2,3,4.	37
Fig. 22 Sample (Hykol with 5% b.w. of glutaraldehyde), five same measurements at 250 Hz	39
Fig. 23. Measuring electrodes covered by aluminum foil + sample on the fabric.....	40
Fig. 24. Blank test (only hykol) and cross-linking at 22°C, for frequencies	41

Fig. 25. Absorbance blank test..... 42

Fig. 26. Absorbance hykol + 6% GTH 42

LIST OF TABLES

Table 1. Hierarchy according to structure and area of usage [1].....	10
Table 2. Percentage volume of main amino acids in	11
Table 3 Time dependence of cross-linking.....	38
Table 4. Absolute values of drop of dissipation factor	41
Table 5. Average absorbance of hykol	44
Table 6. Average absorbance of cross-linked hykol.....	44

LIST OF APPENDICES

Appendix A

- a) Epoxy resin cure – measuring of dissipation factor for temperatures 22°C and 30°C at frequencies 250Hz, 500Hz and 1000Hz
- b) Epoxy resin cure – measuring of dissipation factor for temperatures 40°C and 50°C at frequencies 250Hz, 500Hz and 1000Hz.

Appendix B

- a) Standardized time dependences of dissipation factor during the cross-linking reaction for temperature 22°C for 250Hz and 500Hz. Both plots show four measurements which are labeled 1,2,3,4.
- b) Standardized time dependences of dissipation factor during the cross-linking reaction for temperature 22°C at 1000 Hz and for temperature 30°C at 500 Hz. Both plots show four measurements which are labeled 1,2,3,4.
- c) Standardized time dependences of dissipation factor during the cross-linking reaction for temperature 30°C at 1000Hz and for temperature 40°C at 250Hz. Both plots show four measurements which are labeled 1,2,3,4.
- d) Standardized time dependences of dissipation factor during the cross-linking reaction for temperature 40°C at 500 Hz and 1000 Hz. Both plots show four measurements which are labeled 1,2,3,4.
- e) Standardized time dependences of dissipation factor during the cross-linking reaction for temperature 50°C at 500 Hz and 1000 Hz. Both plots show four measurements which are labeled 1,2,3,4.

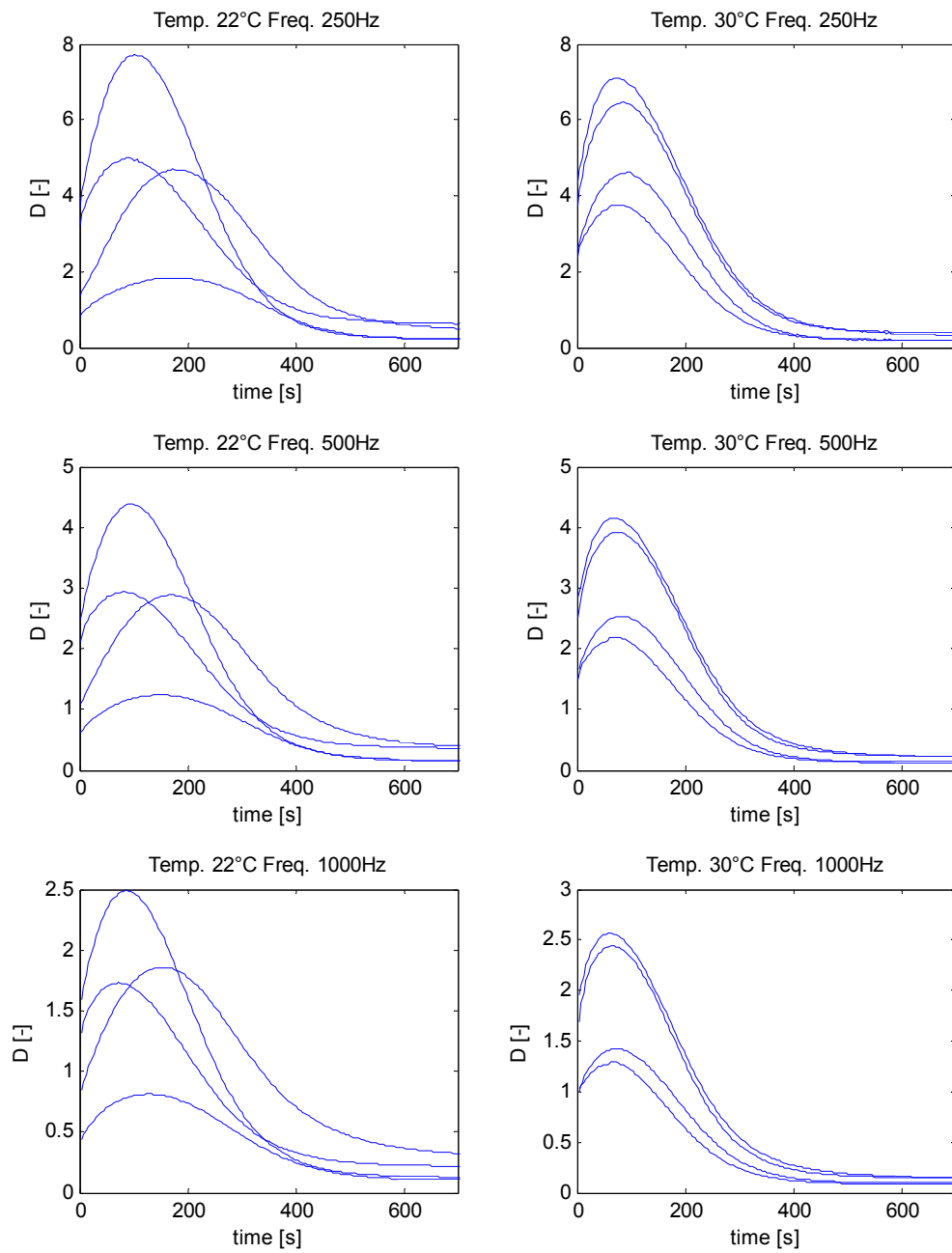
Appendix C

- a) Hykol 65% aqueous solution + GTH 25% aqueous solution
- b) Hykol 65% aqueous solution + GTH 25% aqueous solution

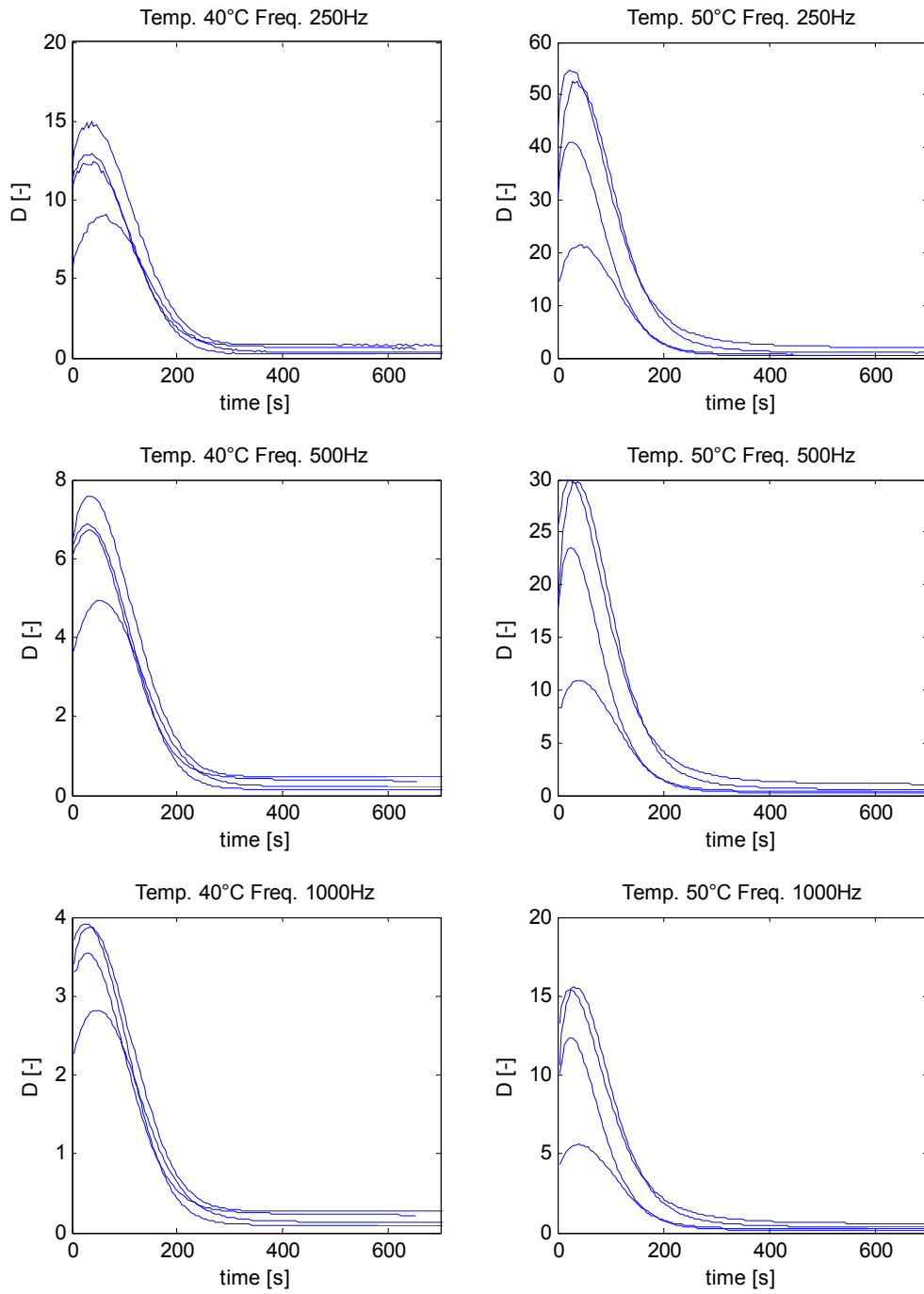
CD

Contains measured data, programs and this work in pdf format.

Appendix A

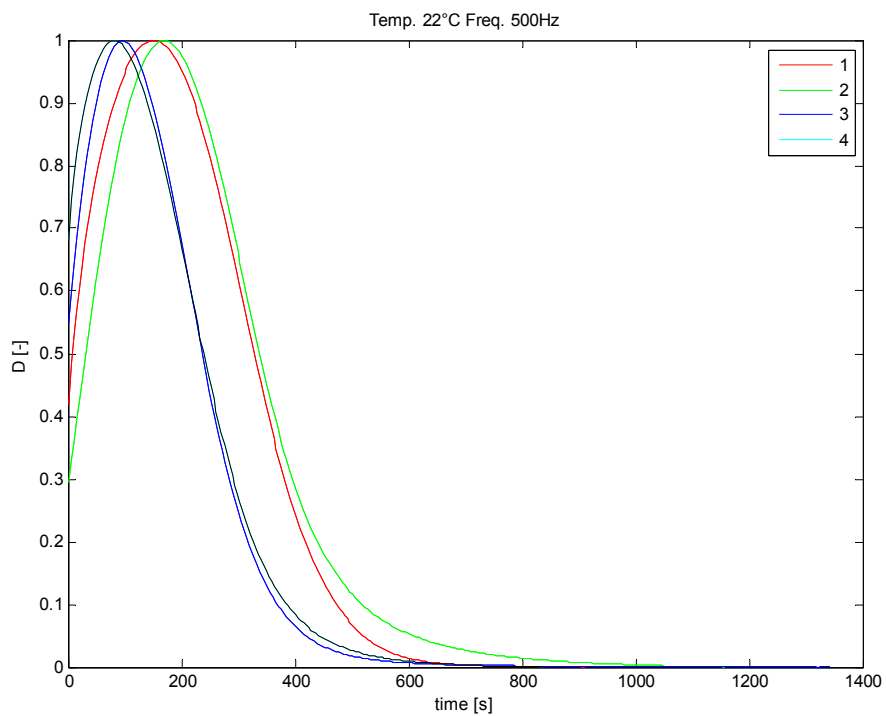
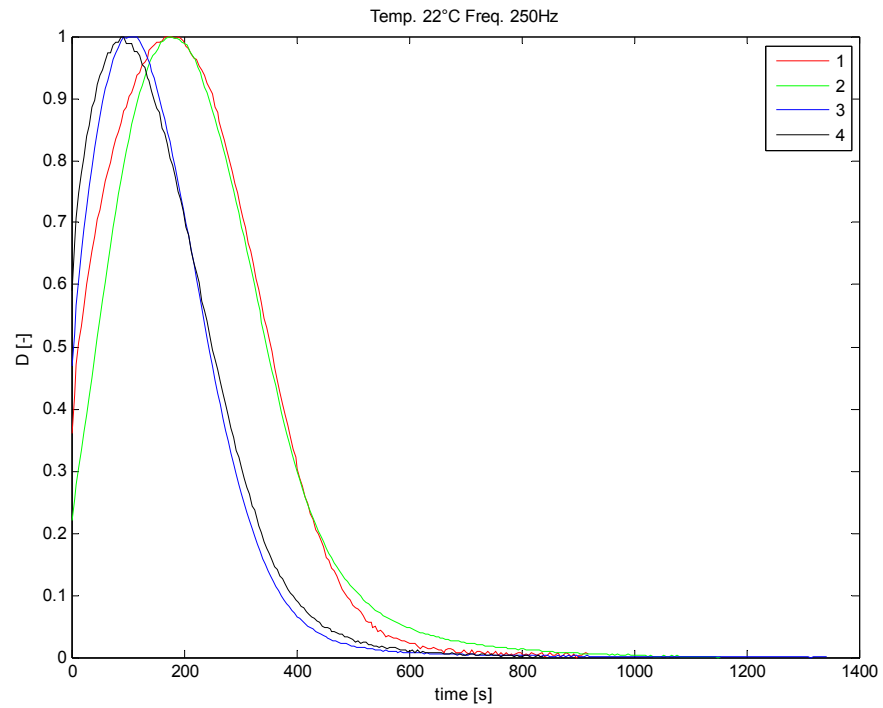


a) Epoxy resin cure – measuring of dissipation factor for temperatures 22°C and 30°C at frequencies 250Hz, 500Hz and 1000Hz

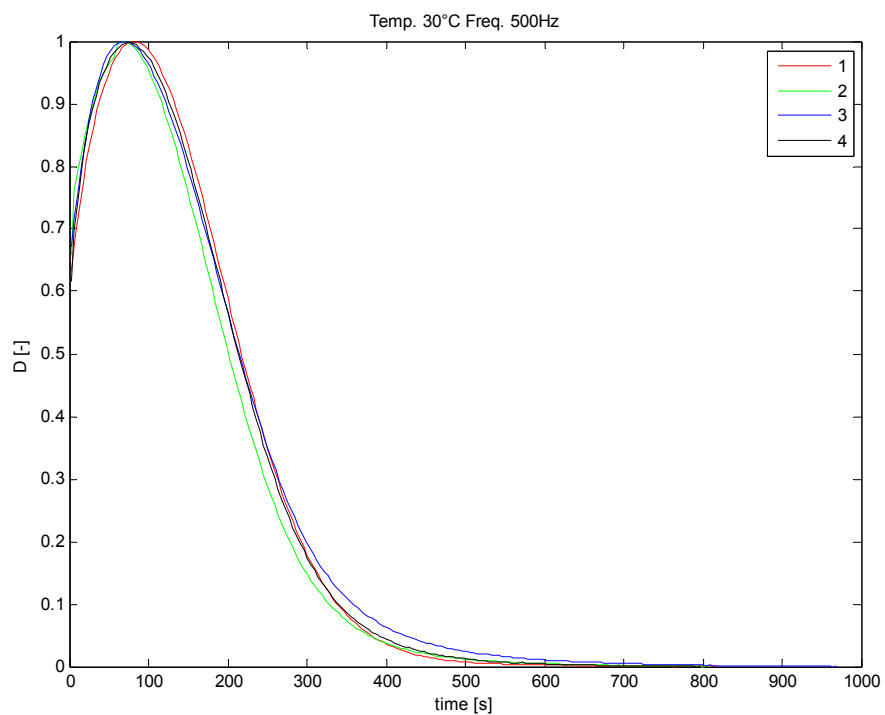
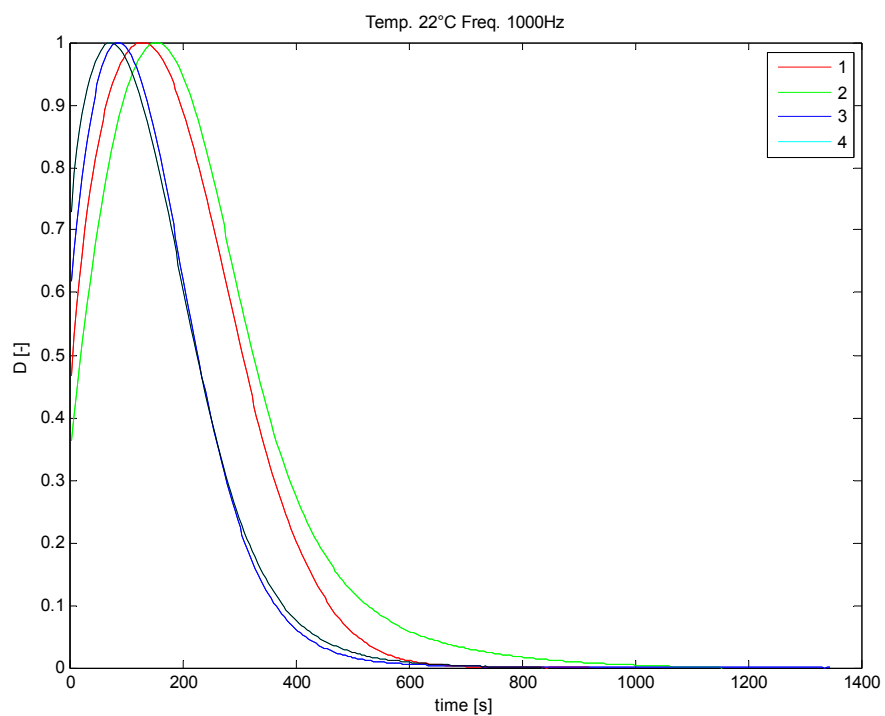


b) Epoxy resin cure – measuring of dissipation factor for temperatures 40°C and 50°C at frequencies 250Hz, 500Hz and 1000Hz.

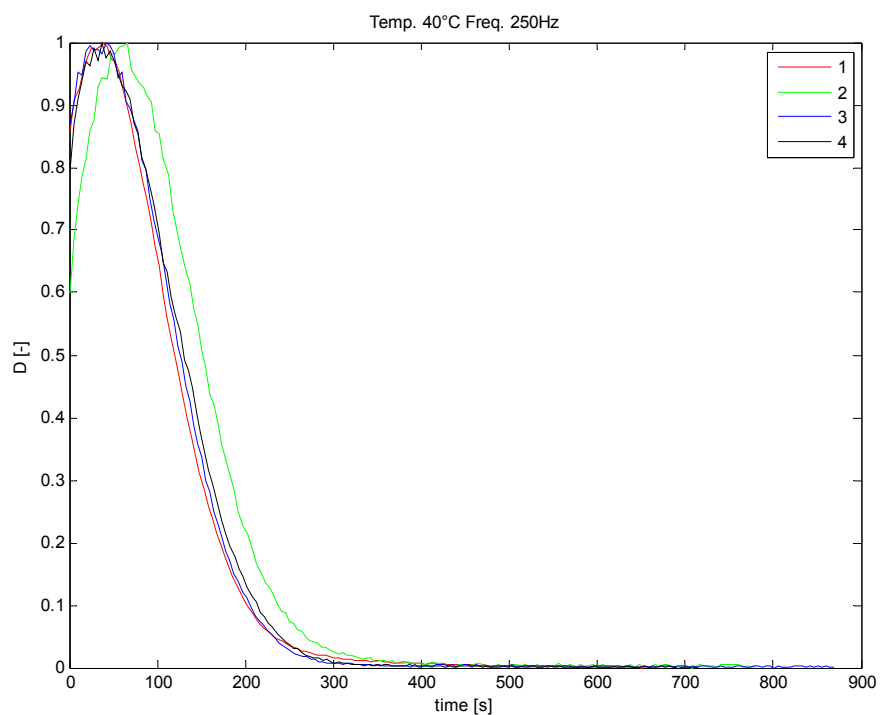
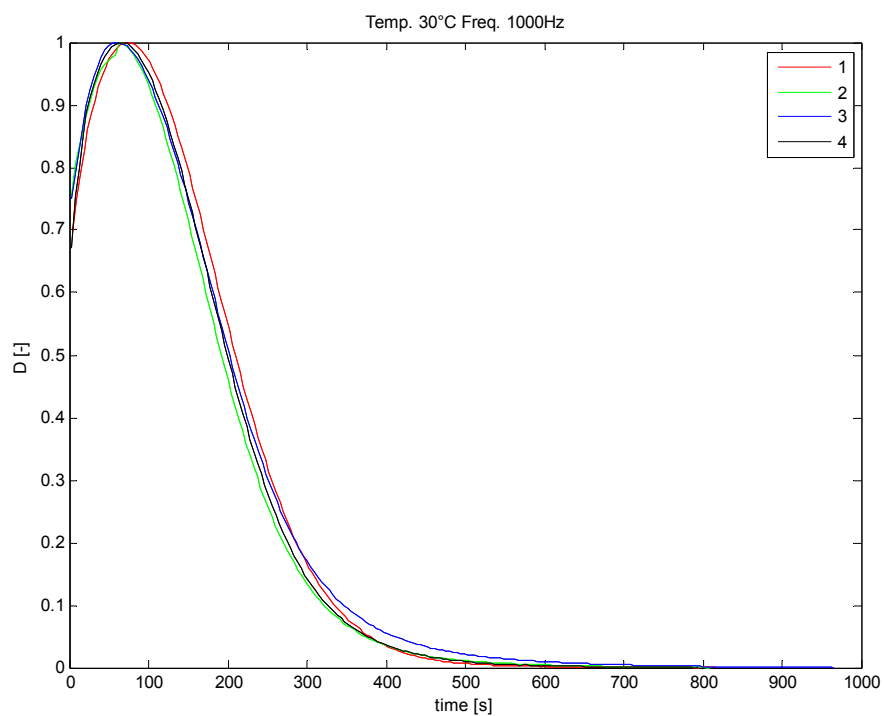
Appendix B



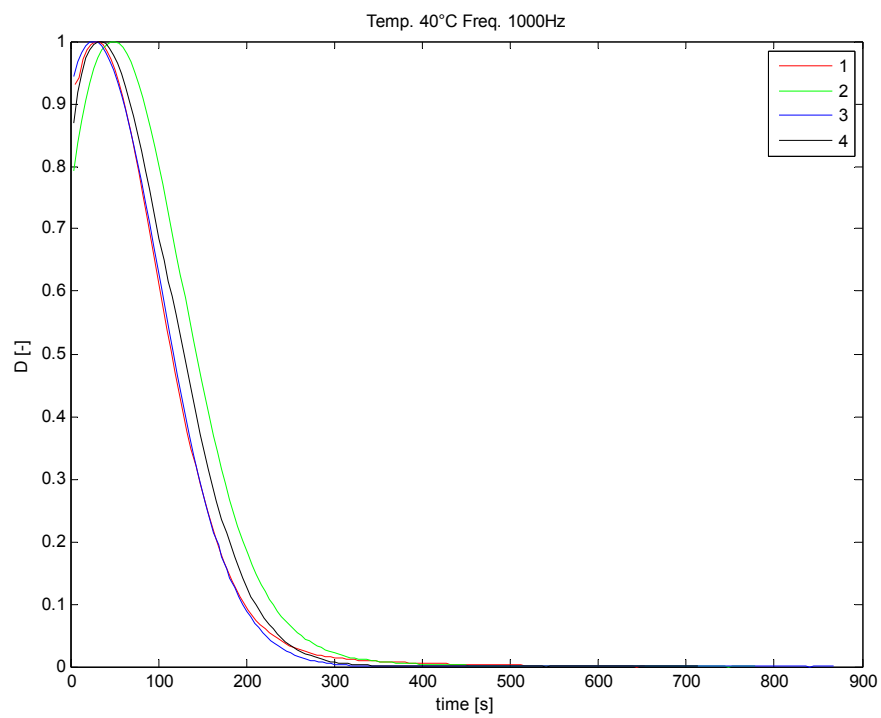
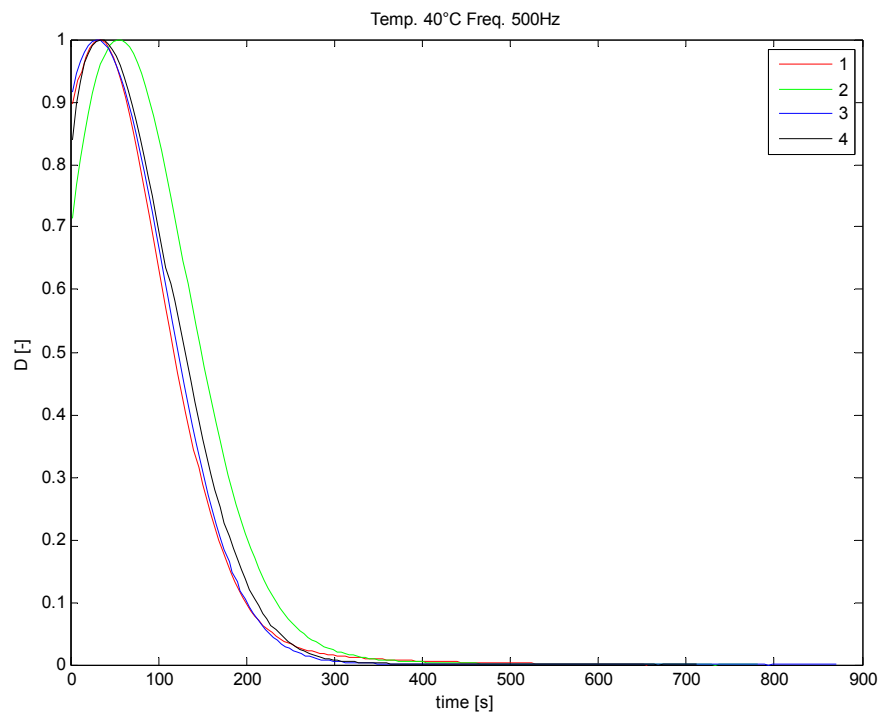
- a) Standardized time dependences of dissipation factor during the cross-linking reaction for temperature 22°C for 250Hz and 500Hz. Both plots show four measurements which are labeled 1,2,3,4.



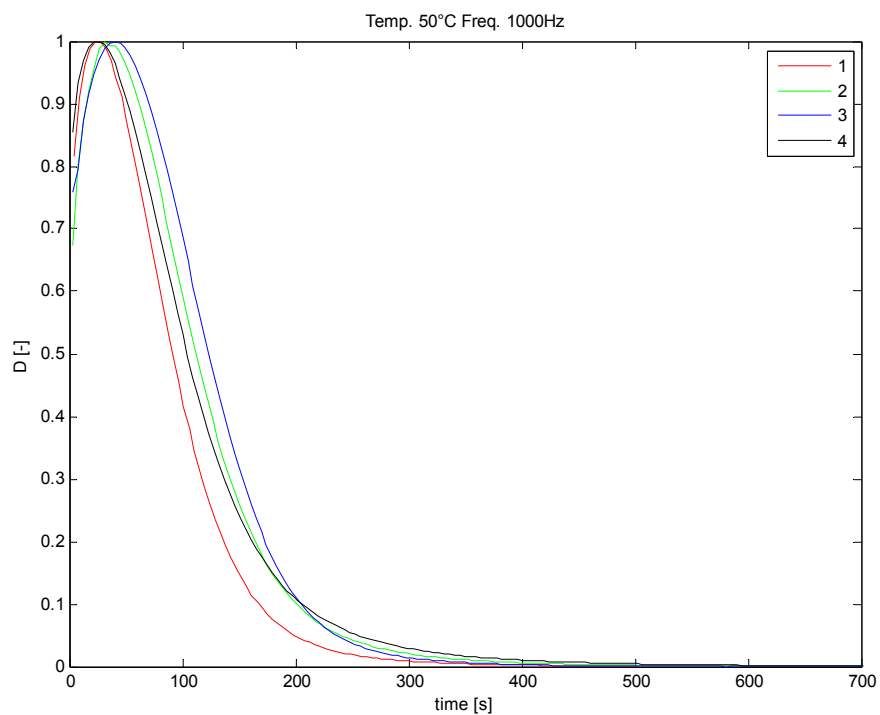
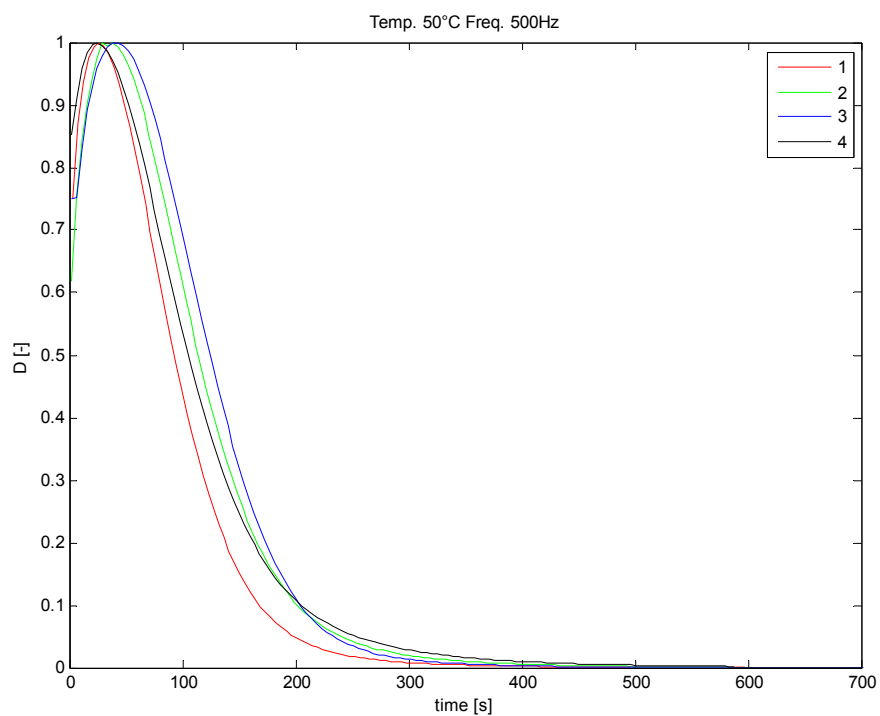
b) Standardized time dependences of dissipation factor during the cross-linking reaction for temperature 22°C at 1000 Hz and for temperature 30°C at 500 Hz. Both plots show four measurements which are labeled 1,2,3,4.



c) Standardized time dependences of dissipation factor during the cross-linking reaction for temperature 30°C at 1000Hz and for temperature 40°C at 250Hz. Both plots show four measurements which are labeled 1,2,3,4.

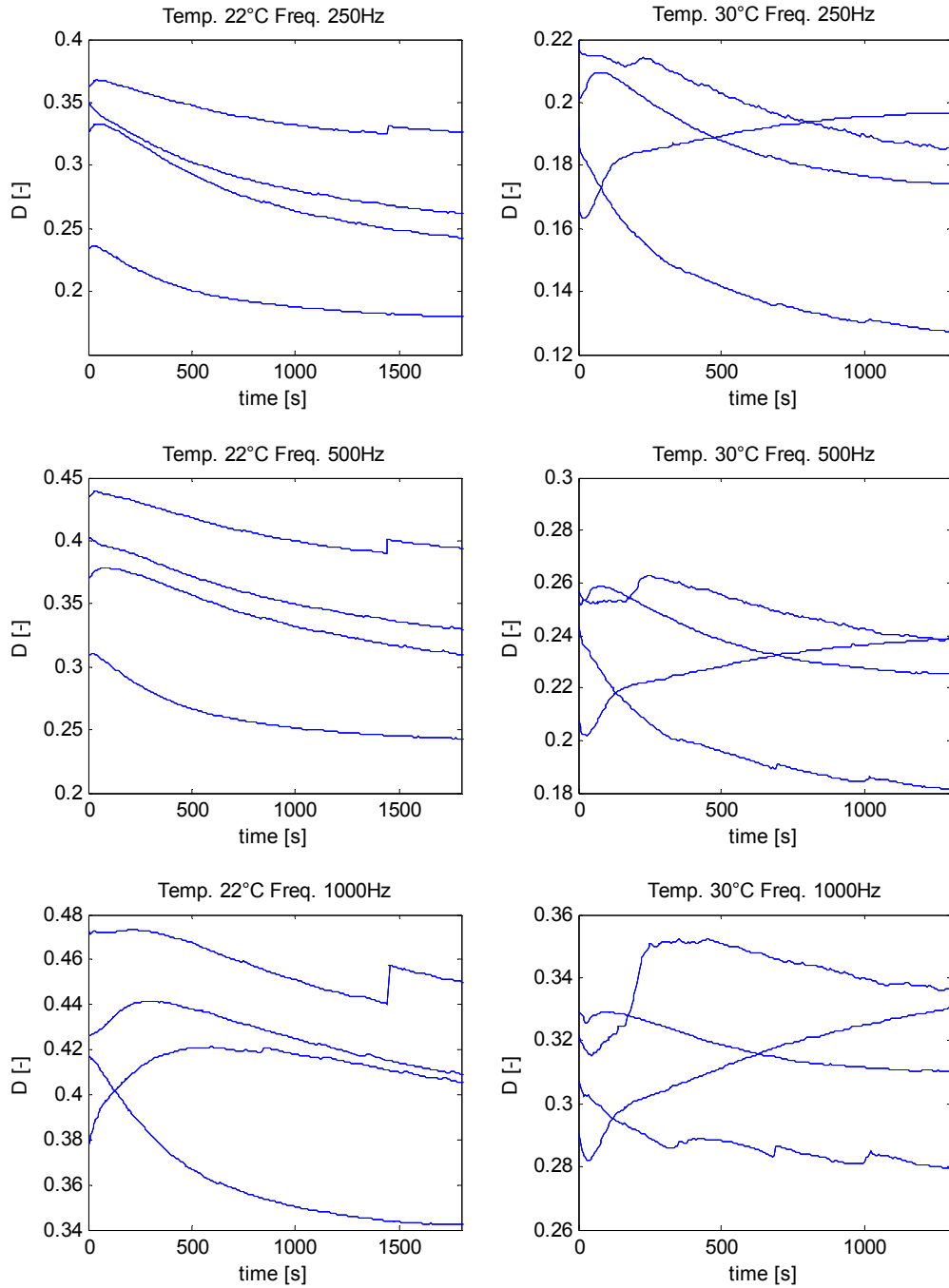


d) Standardized time dependences of dissipation factor during the cross-linking reaction for temperature 40°C at 500 Hz and 1000 Hz. Both plots show four measurements which are labeled 1,2,3,4.

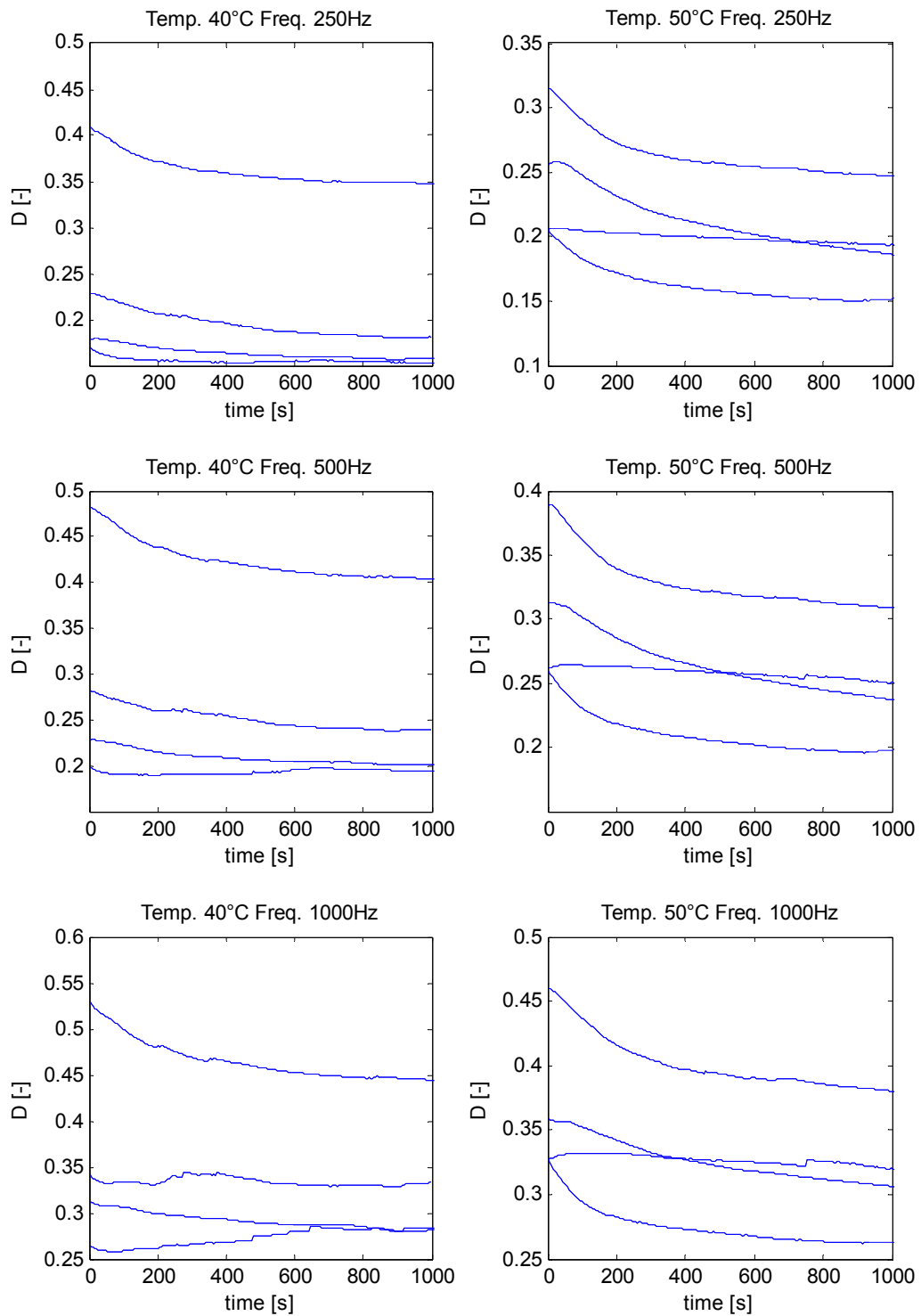


e) Standardized time dependences of dissipation factor during the cross-linking reaction for temperature 50°C at 500 Hz and 1000 Hz. Both plots show four measurements which are labeled 1,2,3,4.

Appendix C



a) Hykol 65% aqueous solution + GTH 25% aqueous solution



b) Hykol 65% aqueous solution + GTH 25% aqueous solution